Regional characteristics of atmospheric sulfate formation in East Antarctica imprinted on 17O-excess signature

Sakiko Ishino, Shohei Hattori, Michel Legrand, Q. Chen, Becky Alexander, J. Shao, J. Huang, L. Jaeglé, Bruno Jourdain, Suzanne Preunkert, et al.

Regional characteristics of atmospheric sulfate formation in East Antarctica imprinted on ^{17}O-excess signature

S. Ishino[1,2], S. Hattori[1], M. Legrand[3], Q. Chen[4], B. Alexander[4], J. Shao[4,5], J. Huang[4], L. Jaegle[4], B. Jourdain[3], S. Preunkert[3], A. Yamada[6], N. Yoshida[1,7], and J. Savarino[3]

[1]Department of Chemical Science and Engineering, School of Materials and Chemical Technology, Tokyo Institute of Technology, Yokohama 226-8503, Japan

[2]National Institute of Polar Research, Research Organization of Information and Systems, Tokyo 190-8518, Japan

[3]Univ. Grenoble Alpes, CNRS, IRD, Grenoble INP, Institut des Géosciences de l'Environnement (IGE), Grenoble 38058, France

[4]Department of Atmospheric Sciences, University of Washington, Seattle, WA 98195, USA

[5]College of Flight Technology, Civil Aviation University of China, Tianjin 300300, China.

[6]Toshima Electric Ltd., Tokyo 170-0005, Japan

[7]Earth-Life Science Institute, Tokyo Institute of Technology, Tokyo 152-8551, Japan.

Corresponding author: Shohei Hattori (hattori.s.ab@m.titech.ac.jp)

Key Points:

- Regional characteristics of atmospheric sulfate formation were probed by ^{17}O-excess (Δ^{17}O) of sulfate at inland and coastal East Antarctica.
- Specifically high Δ^{17}O in spring–summer at inland suggests that chemical destruction of methanesulfonate (MS^-) on the Antarctic Plateau produces sulfate.
- Existing gap between Δ^{17}O of sulfate in the atmosphere and ice can be reconciled by MS^- destruction in snow.

Abstract

^{17}O-excess ($\Delta^{17}O = \delta^{17}O - 0.52 \times \delta^{18}O$) of sulfate trapped in Antarctic ice cores has been proposed as a potential tool for assessing past oxidant chemistry, while insufficient understanding of atmospheric sulfate formation around Antarctica hampers its interpretation. To probe influences of regional specific chemistry, we compared year-round observations of $\Delta^{17}O$ of non-sea-salt sulfate in aerosols ($\Delta^{17}O(SO_4^{2-})_{nss}$) at Dome C and Dumont d'Urville, inland and coastal sites in East Antarctica, throughout the year 2011. Although $\Delta^{17}O(SO_4^{2-})_{nss}$ at both sites showed consistent seasonality with summer minima (~1.0 ‰) and winter maxima (~2.5 ‰) owing to sunlight-driven changes in the relative importance of O_3-oxidation to OH- and H_2O_2-oxidation, significant inter-site differences were observed in austral spring–summer and autumn. The co-occurrence of higher $\Delta^{17}O(SO_4^{2-})_{nss}$ at inland (2.0 ± 0.1 ‰) than the coastal site (1.2 ± 0.1 ‰) and chemical destruction of methanesulfonate (MS^-) in aerosols at inland during spring–summer (October to December), combined with the first estimated $\Delta^{17}O(MS^-)$ of ~16 ‰, implies that MS^- destruction produces sulfate with high $\Delta^{17}O(SO_4^{2-})_{nss}$ of ~12 ‰. If contributing to the known post-depositional decrease of MS^- in snow, this process should also cause a significant post-depositional increase in $\Delta^{17}O(SO_4^{2-})_{nss}$ over 1 ‰, that can reconcile the discrepancy between $\Delta^{17}O(SO_4^{2-})_{nss}$ in the atmosphere and ice. The higher $\Delta^{17}O(SO_4^{2-})_{nss}$ at the coastal site than inland during autumn (March to May) may be associated with oxidation process involving reactive bromine and/or sea-salt particles around the coastal region.

Plain Language Summary

It has been proposed that the past variations of atmospheric oxidants (e.g., ozone) might be estimated using ^{17}O-excess, an unique isotopic signature, of sulfate trapped in polar ice cores. However, chemical processes altering ^{17}O-excess of sulfate in the atmosphere and also in snow after deposition has not been fully understood, limiting the practicality of the signature. We investigated regional differences in ^{17}O-excess of sulfate in aerosol particles at inland and coastal sites in East Antarctica. Our results suggest that the chemical destruction of atmospheric methanesulfonate, the second abundant sulfur compound in Antarctic aerosols, produces sulfate with significantly high ^{17}O-excess signature at inland Antarctica. If also occurring in snow, this process can explain the existing gap of the signature between the atmosphere and ice. These results should be taken into account through future studies investigating the past atmospheric compositions using this signature in ice cores.

1 Introduction

Sulfate is a major component of impurities trapped in Antarctic ice cores and widely used for reconstruction of paleoclimate conditions (e.g., Legrand and Mayewski, 1997). For instance, since the main source of sulfate in Antarctica is oxidation of dimethyl sulfide (DMS) emitted by marine biota (Minikin et al., 1998; Cosme et al., 2005), sulfate in the Antarctic ice cores are often discussed in light of the past bioproductivity of the Southern Ocean (Legrand et al., 1988; Wolff et al., 2006; Azuma et al., 2019). In addition to the use of sulfate content in ice cores, ^{17}O-excess ($\Delta^{17}O = \delta^{17}O - 0.52 \times \delta^{18}O$) of sulfate ($\Delta^{17}O(SO_4^{2-})$) is expected to be a potential tool assessing past oxidant chemistry involving ozone (O_3) and hydroxyl radicals (OH), those playing central roles in tropospheric chemistry but not directly preserved in ice cores

(Alexander and Mickley, 2015; Kunasek et al., 2010; Sofen et al., 2014; Murray et al., 2014). $\Delta^{17}O(SO_4^{2-})$ is generally assumed to reflect relative importance of different sulfate formation pathways, since the sulfate produced via gas-phase oxidation of SO_2 by OH possesses $\Delta^{17}O = 0$ ‰ (Dubey et al., 1997; Barkan and Luz, 2005), whereas those produced via aqueous-phase oxidations of dissolved SO_2 ($S(IV) = SO_2 \cdot H_2O + HSO_3^- + SO_3^{2-}$) by O_3 or hydrogen peroxide (H_2O_2) possess $\Delta^{17}O > 0$ ‰ (Savarino et al., 1999, 2000; Vicars and Savarino, 2014). Sofen et al. (2014) observed a 1.1 ‰ increase of $\Delta^{17}O(SO_4^{2-})$ within the early 19th century in West Antarctic Ice Sheet Divide ice cores, probably suggesting an increase of O_3-oxidation relative to OH- and H_2O_2-oxidation in sulfate formation in the mid- to high-southern latitude region. However, they estimated by their box model that a 1.1 ‰ increase of $\Delta^{17}O(SO_4^{2-})$ requires a 260% increase of relative abundance of O_3/OH, which they concluded was highly implausible given a 26% increase of O_3/OH from a chemistry transport model estimate for the Southern Hemisphere extra-tropics. Based on such results, they pointed out deficiencies in the understanding of sulfate formation other than the recognized SO_2 oxidation by OH, H_2O_2, and O_3. Furthermore, there is increasing evidence for a significant difference between the $\Delta^{17}O(SO_4^{2-})$ in aerosol samples (ca. 1.5 ‰; Hill-Falkenthal et al., 2013; Ishino et al., 2017; Walters et al., 2019) and those in ice-cores corresponding to the present-day climate conditions (ca. 3 ‰; Alexander et al., 2002, 2003; Kunasek et al., 2010; Sofen et al., 2014). Despite the significance of this ~1.5 ‰ shift in $\Delta^{17}O(SO_4^{2-})$ compared to the observed variability in ice cores (1.3–4.8 ‰ for glacial-interglacial time scale), there has been no study pointing it out so far. Thus, the interpretation of ice-core $\Delta^{17}O(SO_4^{2-})$ records requires a better understanding of atmospheric sulfate formation in Antarctica.

In Antarctica, where the impact of anthropogenic emissions is still insignificant, there exist unique oxidative conditions associated with natural emissions of reactive trace gases from snow and sea-ice surfaces (Grannas et al., 2007; Simpson et al., 2007). One characteristic is drastic enhancements of photochemical oxidants, represented by OH and O_3, over the Antarctic Plateau after polar sunrise to the austral mid-summer (Grannas et al., 2007; Crawford et al., 2001; Mauldin et al., 2001), which is mainly triggered by nitrate photolysis within snowpack (Frey et al., 2009; Erbland et al., 2013; Noro et al., 2018) emitting reactive nitrogen species (e.g., NO_x) to the atmosphere (Davis et al., 2008). It has been recently found that the concentration of methanesulfonate (MS^-), a second abundant product of DMS oxidation after sulfate, suddenly decreased in the highly oxidative atmosphere in mid-summer at Dome C, inland Antarctica (Legrand et al., 2017b). It was hypothesized that this may be due to a chemical destruction of MS^-, possibly into sulfate, but the hypothesis needs confirmation and quantification. Since it is also known that MS^- is partially lost in snow after its deposition (Wagnon et al., 1999; Delmas et al., 2003; Weller et al., 2004), it is important to examine the impact of MS^- destruction on sulfate formation and $\Delta^{17}O(SO_4^{2-})_{nss}$ values in snow and ice. Another characteristic is the elevated reactive bromine over coastal Antartica during austral spring, as indicated from satellite observations of tropospheirc BrO columns (Theys et al., 2011). Hypobromous acids (HOBr), which is produced from the $BrO + HO_2$ reaction, was proposed to represent up to 50% of total sulfate production in the summertime marine boundary layer over the southern ocean (Chen et al., 2016). The contribution of this reaction is thus expected to be also significant in the Antarctic troposphere.

There are only a few reports of $\Delta^{17}O(SO_4^{2-})$ observations in the present Antarctic atmosphere, and little is known about the influence of characteristic oxidation processes in

Antarctica on $\Delta^{17}O(SO_4^{2-})$. $\Delta^{17}O(SO_4^{2-})$ observations of aerosols at three different sites, Dome C (Hill-Falkenthal et al, 2013) and South Pole (Walters et al., 2019) on the Antarctic Plateau and coastal Antarctic station Dumont d'Urville (DDU) (Ishino et al., 2017), show similar seasonality with minima in the austral summer and higher values in the autumn to spring, which likely reflects a seasonal shift from OH- and H_2O_2- to O_3-dominated chemistry. In addition, Ishino et al. (2017) and Walters et al. (2019) suggested the possibility of an increased contribution of S(IV) + HOBr during austral spring at DDU and summer at South Pole, respectively, based on the relatively low $\Delta^{17}O(SO_4^{2-})$ in those seasons. However, the importance of S(IV) + HOBr remains inconclusive, since both results in those two previous works can also be explained by the contribution of OH- and H_2O_2-oxidation. Meanwhile, there is no study investigating the possible impact of MS^- destruction to $\Delta^{17}O(SO_4^{2-})$ so far. To evaluate the consequences of characteristic chemical processes to $\Delta^{17}O(SO_4^{2-})$ in Antarctica, a comparison of the isotope signatures at inland and coastal sites can be helpful, since the MS^- destruction appears most significant on the Antarctic Plateau (Legrand et al., 2017b) while reactive bromine is more abundant in coastal regions (Theys et al., 2011). Here, we conduct an inter-site comparison of year-round $\Delta^{17}O(SO_4^{2-})$ values of atmospheric sulfate, using weekly $\Delta^{17}O(SO_4^{2-})$ observations newly obtained for the inland site Dome C in this study and those previously obtained for coastal site DDU (Ishino et al., 2017) in the same year 2011. We also compare the observations with the $\Delta^{17}O(SO_4^{2-})$ values estimated using a global chemical-transport model GEOS-Chem, which includes reactive bromine production from sea-salt aerosols that originate from both the open ocean and blowing snow sublimation over sea-ice (Huang et al., 2020).

2 Materials and Methods

2.1 Aerosol sampling and measurement of soluble species

Aerosol samples were collected at Dome C (75°10′S, 123°30′E; 3233 m above sea level), located on the East Antarctic Plateau 1100 km from the nearest coast. The aerosol sampling is performed continuously at Dome C from the year 2010 as a part of Sulfate and Nitrate Evolution at Dome C (SUNITEDC) program (e.g., Erbland et al., 2013). Bulk aerosol was collected on glass fiber filters using high-volume air sampler (HVAS; General Metal Works GL 2000H Hi Vol TSP; Tisch Environmental, Cleves, OH, USA) at the flow rate of 1.7 m^3 min^{-1} with time resolution of 1–2 week. The HVAS was placed at ~1 km distant from the main building of research activity at Dome C. A field blank was checked once per month by mounting filters onto the filter holder and running for 1 min. After each collection run, filters were removed from the HVAS and wrapped in aluminium foil, which were sealed in plastic bags, stored at –20 °C, and shipped to Institut des Géosciences de l'Environnement (Grenoble, France) for chemical analyses. Samples collected during January to December 2011 were used in this study.

The procedures for extraction and quantification of soluble species concentrations in aerosols are detailed in Ishino et al. (2019). Some anions (NO_3^-, SO_4^{2-}) and cations (K^+, Mg^{2+}, Ca^{2+}) were measured at Tokyo Tech using ion chromatograph ICS2100, DIONEX with a guard column (Dionex IonPac AG19) and a separation column (Dionex IonPac AS19) for anions, and 881 Compact IC Pro, Metrohm with a guard column (Metrosep C4 S-Guard/4.0) and a separation column (Metrosep C 4-150/4.0) for cations. Considering high blank loading on filters or the lack

of ion standard materials at Tokyo Tech., the concentration of other ions (MS^-, Cl^-, Br^-, oxalate ($C_2O_4^{2-}$), and Na^+) were obtained from other aerosol samples as described in Legrand et al. (2017a, 2017b). The measured ion concentrations were corrected for blank values, and reported as atmospheric concentration in standard temperature and pressure (T = 273.15 K, p = 101325 Pa) based on meteorological data of Dome C provided by IPEV/PNRA (www.climantartide.it). The uncertainties were estimated based on the typical uncertainty of the ion chromatography analysis (5%).

2.2 Oxygen isotope measurements of sulfate ($\Delta^{17}O(SO_4^{2-})$)

$\Delta^{17}O(SO_4^{2-})$ values were measured with an isotope ratio mass spectrometer (IRMS) (MAT253; Thermo Fisher Scientific, Bremen, Germany), coupled with an in-house measurement system built following original setup by Savarino et al. (2001) and a series of improvements (Schauer et al., 2012; Geng et al., 2013). The detailed method is described in Ishino et al. (2017). Briefly, ca. 1 μmol of SO_4^{2-} was separated from other anions using ion chromatography, and chemically converted to silver sulfate (Ag_2SO_4) using ion exchange resin. O_2 produced via thermal decomposition of the Ag_2SO_4 at 1000 °C within a high temperature conversion elemental analyzer (TC/EA; Thermo Fisher Scientific, Bremen, Germany) was analysed for isotopic compositions with the IRMS system. The inter-laboratory calibrated standards (Sulf-α, β and ε; Schauer et al., 2012) were used to assess the accuracy of our measurements of our working standards. Measured $\Delta^{17}O(SO_4^{2-})$ was corrected for oxygen isotope exchange with quartz ($\Delta^{17}O$ = 0 ‰; Matsuhisa et al., 1978) by estimating the magnitude of isotopic exchange based on the set of working standard measurements along with the sample measurement runs as described in Schauer et al. (2012). The precision (1σ) of corrected $\Delta^{17}O$ was ± 0.2 ‰ based on replicate analyses (n = 35) of our working standard C ($\Delta^{17}O$ = 8.4 ‰).

Since sea-salt sulfate aerosols (ss-SO_4^{2-}) are not impacted by atmospheric oxidation processes (i.e., $\Delta^{17}O(SO_4^{2-})_{ss}$ = 0 ‰), both total sulfate concentrations and $\Delta^{17}O$ values were corrected for their ss-SO_4^{2-} component to obtain their non-sea-salt sulfate (nss-SO_4^{2-}) content, using the following Eq. (1) and (2).

$$[SO_4^{2-}]_{nss} = [SO_4^{2-}]_{total} - k \times [Na^+] \quad (1)$$

$$\Delta^{17}O(SO_4^{2-})_{nss} = \frac{[SO_4^{2-}]_{total}}{[SO_4^{2-}]_{nss}} \times \Delta^{17}O(SO_4^{2-})_{total} \quad (2)$$

where "total" is the sum of ss- and nss-SO_4^{2-} components; and k is the mass ratio of $[SO_4^{2-}]_{ss}/[Na^+]$ in seawater (0.25; Holland et al., 1986). To take into account sea salt chemical fractionation processes that occurs in the Antarctic region in winter, when temperatures drop below −8 °C in the presence of sea-ice (Wagenbach et al., 1998), k value of 0.16 ± 0.05 (Legrand et al., 2017a) was applied from May to October. Eq. (2) represents the isotope mass balance equation between ss- and nss-SO_4^{2-}, with $\Delta^{17}O(SO_4^{2-})_{ss}$ = 0 ‰. Note that the sea salt fractionation is a chemical fractionation and should not shift $\Delta^{17}O$. The uncertainties of ion concentration measurement (± 5%), $\Delta^{17}O$ measurement (± 0.2 ‰), and the k value were propagated to $\Delta^{17}O(SO_4^{2-})_{nss}$. The obtained uncertainty of $\Delta^{17}O(SO_4^{2-})_{nss}$ was ± 0.3 ‰ on average, while reaches ± 1.1 ‰ at maximum in the austral mid-winter when the $[SO_4^{2-}]_{nss}/[SO_4^{2-}]_{total}$ is minimum.

2.3 Complementary data

The $\Delta^{17}O(SO_4^{2-})_{nss}$ at Dome C were compared to those previously obtained at DDU (Ishino et al., 2017) in the same year 2011. The inter-site difference was evaluated at weekly resolution by subtracting the $\Delta^{17}O(SO_4^{2-})_{nss}$ of each DDU sample from that of each Dome C sample collected in the closest time period, hereafter denoted Δ_{DC-DDU}. Note that, at DDU, aerosol samples were collected separately for coarse (>1 μm) and fine (<1 μm) mode particles and the $\Delta^{17}O(SO_4^{2-})_{nss}$ was measured for fine mode (Ishino et al., 2017). The results were also compared to datasets of oxidants available year-round at both Dome C and DDU, O_3 mixing ratios (Legrand et al., 2016a) and an estimate of total gaseous inorganic bromine ($[Br_y^*]$ = [HBr] + [HOBr] + 0.9[Br_2] + 0.4[BrO] + [$BrNO_2$] + [$BrONO_2$] + [Br]) (Legrand et al., 2016b), as indicators of regional characterictic processes. Furthermore, $[MS^-]/[SO_4^{2-}]_{nss}$ mass ratios at Dome C (Legrand et al., 2017b) and DDU (Ishino et al., 2017) for the same year were used to examine the influence of chemical destruction of MS^- on sulfate formation in the mid-summer.

Additionally, to explore other possible processes influencing the $\Delta^{17}O(SO_4^{2-})_{nss}$ values, we investigated the relationship of Δ_{DC-DDU} to various chemical species observed at both sites. They include ion concentrations and acidity in aerosols ($[H^+]$), ratios of respective sulfur components, $[SO_4^{2-}]_{ss}/[SO_4^{2-}]_{total}$ ratio (= 1 – $[SO_4^{2-}]_{nss}/[SO_4^{2-}]_{total}$, cf., Eq. (1)), and sulfur isotopic composition of non-sea-salt sulfate ($\delta^{34}S_{nss}$) (Ishino et al., 2019). $[H^+]$, estimated by using the following equation, was used to consider the contribution of aqueous-phase S(IV) + O_3 pathway, which is highly dependent on pH of liquid water in the atmosphere (Seinfeld and Pandis, 2006).

$$[H^+] = ([Cl^-] + [Br^-] + [NO_3^-] + 2[SO_4^{2-}] + 2[C_2O_4^{2-}]) - ([Na^+] + [NH_4^+] + [K^+] + 2[Mg^{2+}] + 2[Ca^{2+}]) \quad (3)$$

Also $[SO_4^{2-}]_{ss}/[SO_4^{2-}]_{total}$ was used to consider the potential importance of aqueous-phase S(IV) + O_3 reaction, since it has been recognized that S(IV) + O_3 proceeds rapidly in alkaline (pH ~ 8) deliquescent solution in fresh sea-salt particles, subsequently shutting off due to acidification of sea salt aerosol by the produced sulfate as well as by uptake of acidic gases such as SO_2, HNO_3, and H_2SO_4 (Alexander et al., 2005). $\delta^{34}S_{nss}$ was used to test the impact of sulfur sources on $\Delta^{17}O(SO_4^{2-})_{nss}$, since it reflects the relative contributions of marine biogenic (i.e., DMS-sourced) sulfate and non-marine sulfate (nmb-SO_4^{2-}) including volcanic and continental sulfur sources (Patris et al., 2000; Pruett et al., 2004; Ishino et al., 2019). Additionally, ^{210}Pb was used to trace the contribution of long-range transport of continental submicron aerosols (Elsasser et al., 2011; Legrand et al., 2017b). The relationships were examined separately for each season: December-January-February (DJF), March-April-May (MAM), June-July-August (JJA), September-October-November (SON), as well as October 29th to December 23rd (OND), where the last one was defined based on the specifically positive Δ_{DC-DDU} values as explained later in Section 3.1. The obtained correlation coefficients (*r* and *p* values) are summarized in Table S1.

2.4 Model description and limitations

We used v11-02d of the GEOS-Chem global chemical-transport model of coupled aerosol-oxidant chemistry (Park et al., 2004; http://www.geos-chem.org/) to estimate the relative importance of sulfate formation processes and $\Delta^{17}O(SO_4^{2-})_{nss}$ in Antarctica. The model was run

at 4° × 5° (latitude × longitude) horizontal resolution and 47 vertical levels up to 0.01 hPa, using the MERRA-2 assimilated meteorological data developed by the Global Modeling and Assimilation Office (GMAO) at NASA Goddard Space Flight Center. Simulations were performed for January to December 2011 after spinning up the model for 6 months prior to January 2011.

GEOS-Chem v11-02d includes detailed bromine chemistry as described in Parrella et al., (2012), Schmidt et al. (2016), Sherwen et al. (2016a, 2016b), and Chen et al. (2017). We also applied the reactive bromine emission scheme from sea-salt aerosols produced by blowing snow sublimation over sea-ice as described in Huang et al. (2018, 2020), with surface snow salinity of 0.1 psu and 0.03 psu over the Arctic and the Antarctic, reapectively, for both first-year-ice and multi-year-ice. We assumed an enrichment factor of 9 for Br^-/Na^+ ratio in surface snow on sea-ice relative to seawater. Sea-salt emission from open ocean is simulated as a function of sea surface temperature and wind speed (Jaeglé et al., 2011), with updates from Huang and Jaeglé (2017) for cold ocean waters (SST < 5°C). The model is able to reproduce observed Br_y^* concentrations at DDU from winter to spring (June to November), within the range of standard deviations of the monthly mean observations (Legrand et al., 2016b; Fig. S1). DMS emission is parameterized as a function of sea surface temperature, wind speed, and DMS concentration in seawater obtained from Lana et al. (2011). Note that the model does not include reactive nitrogen emissions from snow nitrate photolysis (Grannas et al., 2007). This would lead to underestimates in oxidants over large area of the Antarctic continents, as exhibited by the underestimates in surface O_3 concentrations at both Dome C and DDU by a factor of ~1.5 (Fig. 1e). Zatko et al. (2016) previously simulated that the inclusion of their snow NO_x emission scheme in GEOS-Chem model will increase surface O_3 concentrations over the Antarctic continent by factors of 1.1–1.8. It is also recently pointed out that the underestimaes in O_3 over the Southern Ocean is improved by the inclusion of a new O_3 deposition scheme associated with chemical reaction of O_3 with iodide on the ocean surface (Pound et al., 2020), which is not implemented in this study. Thus, the model has limitations in reproducing oxidants abundances, even though the general seasonality in O_3 with increases in winter and decreases in summer was reproduced (Fig. 1e). We therefore note that our estimates in the relative contributions of sulfate formation processes bear an uncertainty associated with oxidant abundances despite good reproducibilities in $\Delta^{17}O(SO_4^{2-})_{nss}$ as shown later in Section 3.2 (Fig. 2). The further precise prediction of $\Delta^{17}O(SO_4^{2-})_{nss}$ will require improvements in oxidants reproducibility in the future.

This version of the model includes gas phase oxidation of SO_2 by OH, in-cloud aqueous phase oxidations of S(IV) by H_2O_2, O_3 (Park et al., 2004), and HOBr (Chen et al., 2017), and oxidation of S(IV) by O_3 on sea salt particles (Alexander et al., 2005). For in-cloud reactions, the cloud fraction and the liquid water content of cloud are obtained from MERRA-2 meteorological fields. For pH-dependent reactions such as in-cloud S(IV) + O_3 and S(IV) + HOBr, the effect of heterogeneity of cloud pH on S(IV) partitioning is accounted as described in Alexander et al. (2012). The model assumes in-cloud sulfate formations are prohibited at temperature < –15°C as originally designed by Park et al. (2004). We confirmed that this assumption limits the annual tropospheric sulfate production via aqueous-phase reactions to 13.8 Gg-S on the Antarctic Plateau (> 68°S) in contrast to 137.0 Gg-S on the Southern Ocean (60–68°S) within longitudes of 0–180°E (Fig. S3). This result is consistent with the limited occurrence frequency of super-cooled-liquid-water containing cloud (0–10%) over the Antarctic Plateau compared to over the Southern Ocean (20–60%) (Listowski et al., 2019). S(IV) + O_3 in sea-salt is assumed as a function of SO_2 transfer rate constant from the gas to the aerosol phase, because the rate limiting

step is not the aqueous-phase reaction rate of S(IV) + O_3 in alkaline solution on fresh sea-salt but is gas-phase diffusion of SO_2 to the aerosol surface (Alexander et al., 2005). This reaction is calculated only within MBL column, where the newly emitted sea-salt is available, assuming that sea-salt alkalinity is rapidly consumed by this reaction in addition to the uptake of gas form H_2SO_4 and HNO_3 (Alexander et al., 2005).

We modified the model to tag sulfate produced via each oxidation pathway as different tracers which are transported, as originally described in Alexander et al. (2005). As atmospheric SO_2 rapidly attains isotopic equilibrium with H_2O ($\Delta^{17}O$ = 0 ‰) (Barkan and Luz, 2005; Holt et al., 1981), $\Delta^{17}O$ value of sulfate produced via each formation pathway is determined by $\Delta^{17}O$ value of corresponding oxidant and their transferring factors (Savarino et al., 2000). Since OH also efficiently exchanges its oxygen isotopes with water vapor (Dubey et al., 1997), $\Delta^{17}O(OH)$ is also 0 ‰ under regions where water vapor is abundant (e.g., throughout most of the troposphere) (Lyons, 2001; Morin et al., 2007). Therefore, gas-phase SO_2 + OH produces sulfate with $\Delta^{17}O(SO_4^{2-})$ is assumed to be 0 ‰. Note that it has been previously suggested that $\Delta^{17}O(OH)$ can be 1–3 ‰ at Dome C (Savarino et al., 2016) due to the limited availability of water vapor in inland Antarctica. We also conducted the calculation with $\Delta^{17}O(OH)$ = 3 ‰ as a maximum case, which is expected to produce sulfate with $\Delta^{17}O(SO_4^{2-})$ = 0.75 ‰ with assuming oxygen atom transferring factor of 0.25. We note that there remains possibility that $\Delta^{17}O(OH)$ is higher than 3 ‰ (Savarino et al., 2016), that might cause underestimates in $\Delta^{17}O(SO_4^{2-})_{nss}$. The $\Delta^{17}O(SO_4^{2-})$ value of sulfate produced via aqueous-phase S(IV) + H_2O_2 is assumed to be 0.8 ± 0.2 ‰ based on $\Delta^{17}O(H_2O_2)$ of 1.6 ± 0.3 ‰ (Savarino and Thiemens, 1999) with a transferring factor of 0.5 (Savarino et al., 2000). Note that the $\Delta^{17}O(H_2O_2)$ is derived from only one set of observations at La Jolla, California, and thus needs further verification in various environment in the future. For $\Delta^{17}O(O_3)$, among the whole sets of observations to the present, the two early studies using cryogenic technique had shown large variabilities (24.7 ± 11.4 ‰ and 26.5 ± 5.0 ‰; Krankowsky et al., 1995; Johnston and Theimens, 1997). Such variabilities were much greater than those expected from the experimentally determined pressure and temperature dependency of $\Delta^{17}O(O_3)$, e.g., a decrease of only ~2 ‰ for an pressure increase from 500 to 760 Torr (Morton et al., 1990; Thiemens and Jackson, 1990) and a increase of only ~5 ‰ for an temperature increase from 260 to 320 K (Morton et al., 1990; Janssen et al., 2003). Based on these experimental data, it has been pointed out that these observations would have random errors associated with sampling artifacts (Mauersberger et al., 2003). Therefore, we exclude the data of these two studies from the consideration. Given the consistency of the $\Delta^{17}O(O_3)$ observations using nitrite-coated method among various locations and seasons including at Dome C and DDU (Vicars and Savarino et al., 2014; Savarino et al., 2016; Ishino et al., 2017), we decided to use the average value of the $\Delta^{17}O(O_3)$ observations, which comes to 25.6 ± 1.3 ‰. The $\Delta^{17}O(SO_4^{2-})$ for S(IV) + O_3, both in cloud and in sea salt, is assumed to be 6.4 ± 0.3 ‰, by a transferring factor of 0.25 (Savarino et al., 2000). Since aqueous-phase S(IV) oxidation by HOBr gives an oxygen atom from liquid water to produce sulfate (Fogelman et al., 1989; Troy and Margerum, 1991; Liu et al., 2001), the obtained $\Delta^{17}O(SO_4^{2-})$ is expected to be 0 ‰. Therefore, the $\Delta^{17}O(SO_4^{2-})_{nss}$ values in the model were calculated by adding all sulfate isotope tracers following the mass-balance equation:

$$\Delta^{17}O(SO_4^{2-})_{nss} = 0 \cdot F_{SO2+OH} + 0.8 \cdot F_{S(IV)+H2O2} + 6.4 \cdot F_{S(IV)+O3} + 0 \cdot F_{S(IV)+HOBr}, \quad (4)$$

$$F_i = \frac{[SO_4^{2-}]_i}{[SO_4^{2-}]_{SO2+OH} + [SO_4^{2-}]_{S(IV)+H2O2} + [SO_4^{2-}]_{S(IV)+O3} + [SO_4^{2-}]_{S(IV)+HOBr}}, \quad (5)$$

where F_i represents the relative fraction of sulfate produced via each formation pathway i, respective to total sulfate concentration in each model grid. To calculate the $\Delta^{17}O(SO_4^{2-})_{nss}$ values and compare to the observations, the modeled $\Delta^{17}O(SO_4^{2-})_{nss}$ values of each grid including Dome C and DDU were mass-weighted averaged within the planetary boundary layer.

3 Results

3.1 $\Delta^{17}O(SO_4^{2-})_{nss}$ values observed at Dome C and comparison to DDU

Figure 1 shows nss-SO_4^{2-} concentrations ($[SO_4^{2-}]_{nss}$) and $\Delta^{17}O(SO_4^{2-})_{nss}$ at Dome C throughout 2011 in comparison to those previously reported for DDU (Ishino et al., 2017). Note that the concentration data are presented in Ishino et al. (2019). It is well-established that $[SO_4^{2-}]_{nss}$ is enhanced during austral summer and reduced during winter, a seasonality that is driven by marine biogenic emission of DMS (Preunkert et al., 2007, 2008; Legrand et al., 2017b). This seasonal cycle in $[SO_4^{2-}]_{nss}$ is partially intensified by atmospheric dynamics due to enhanced efficiency of meridional long-range transport and the weakened inversion layer on the Antarctic Plateau during summer, as previously suggested by the similar seasonal cycle with ^{210}Pb (Elsässer et al., 2011; Legrand et al., 2017b). $\Delta^{17}O(SO_4^{2-})_{nss}$ show lower values in austral summer and higher values in winter, with monthly-mean values ranging from 1.1 ± 0.1 ‰ in February to 2.5 ± 0.2 ‰ in August, with a mass-weighted annual average of 1.7 ± 0.1 ‰ (Table 1). These trends and values are generally consistent with previous observations at Dome C in 2010 (Hill-Falkenthal et al., 2013) as well as at DDU in 2011 (Ishino et al., 2017).

Figure 1d shows Δ_{DC-DDU}, the differences in weekly $\Delta^{17}O(SO_4^{2-})_{nss}$ values between the two sites in the year 2011. Throughout most of the year, Δ_{DC-DDU} is 0 ‰ within the range of the estimated uncertainty. However, there are two specific time periods exhibiting Δ_{DC-DDU} values different from 0 ‰. One is from October to December, a transition from the austral spring to summer, when a group of positive Δ_{DC-DDU} values ranging 0.4 ± 0.3 ‰ to 1.4 ± 0.3 ‰ are observed. The second is found from March to May, the austral autumn, when negative Δ_{DC-DDU} values ranging –1.4 ± 0.6 ‰ to –0.5 ± 0.3 ‰ are observed. These Δ_{DC-DDU} values different from zero suggest that sulfate at Dome C and DDU experienced different oxidation processes during their transport from source regions. The possible processes corresponding to these Δ_{DC-DDU} values are discussed in Section 4.

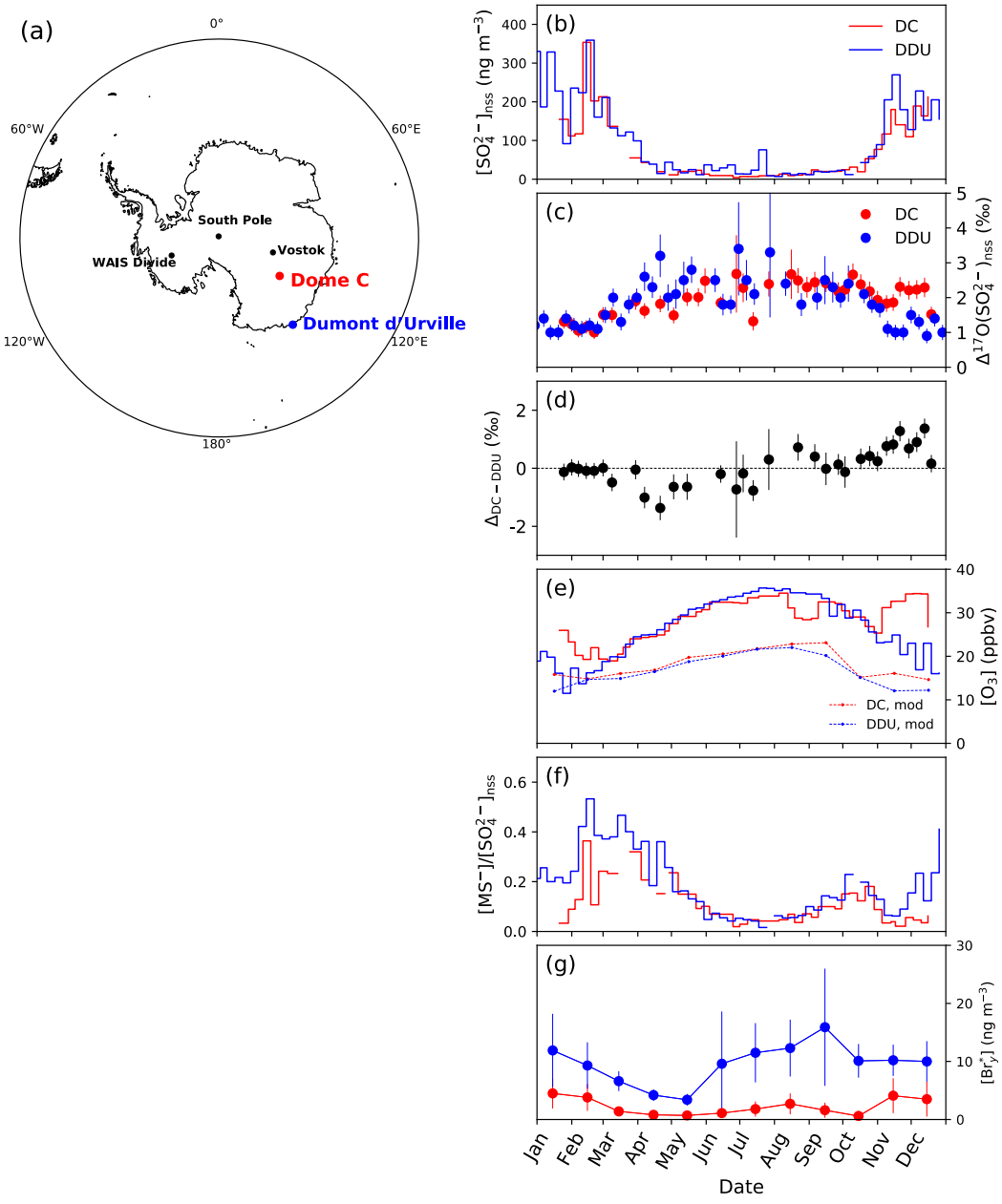

Figure 1. (**a**) Map of stations cited in this study. (**b-g**) Observed seasonal variations of (**b**) non-sea-salt sulfate concentrations, (**c**) $\Delta^{17}O(SO_4^{2-})_{nss}$ values (from this study and Ishino et al., 2017), (**d**) residual $\Delta^{17}O(SO_4^{2-})_{nss}$ values between Dome C and DDU (Δ_{DC-DDU}, see section 3.1), (**e**) ozone mixing ratios (Legrand et al., 2016a), (**f**) $[MS^-]/[SO_4^{2-}]_{nss}$ ratios (Legrand et al., 2017b; Ishino et al., 2017), and (**g**) total gaseous reactive bromine species (Br_y^*) (Legrand et al., 2016b) at Dome C (red) and DDU (blue). Error bars in (**b**) and (**c**) represent the uncertainties propagated from analytical errors of $\Delta^{17}O(SO_4^{2-})_{nss}$ and concentration, and the uncertainty in *k* value ($[SO_4^{2-}]_{ss}/[Na^+]$ mass ratio) in sea-salt. The modeled ozone mixing ratios are also shown in (**d**). The red and blue shaded areas indicate the time periods showing positive and negative Δ_{DC-DDU} values, respectively.

3.2 Modeled sulfate formation processes and $\Delta^{17}O(SO_4^{2-})_{nss}$ values

Figure 2 shows the modeled monthly $[SO_4^{2-}]_{nss}$ and mass-weighted $\Delta^{17}O(SO_4^{2-})_{nss}$ averaged within planetary boundary layer in the model grids including Dome C and DDU, with comparison to the monthly-mean observations (± 1σ). The modeled $[SO_4^{2-}]_{nss}$ reproduces the seasonality of the observations with austral summer maxima and winter minima, but the model overestimates $[SO_4^{2-}]_{nss}$ observations for summer (DJF) and winter (JJA) by a factor of 2 and 4 at Dome C, and 2 and 3 at DDU, respectively. Chen et al. (2018) reported that GEOS-Chem model run with DMS concentration in seawater from Lana et al. (2011) and without DMS oxidation by BrO, the condition used in this study, overestimates mixing ratio of DMS by a factor of 5 and 21 during summer and winter at DDU, respectively. This is likely a main reason for the overestimate of $[SO_4^{2-}]_{nss}$ at DDU and Dome C, as DMS oxidation is thought to be the main source of sulfate in these locations (e.g., Minikin et al., 1998; Ishino et al., 2019). We note that the overestimate of $[SO_4^{2-}]_{nss}$ could lead to an underestimate of $F_{S(IV)+O3}$ and thus $\Delta^{17}O(SO_4^{2-})_{nss}$ in the model as we discuss in Section 4.

The model also reproduces the seasonality of $\Delta^{17}O(SO_4^{2-})_{nss}$ in the observations with austral summer minima and austral winter maxima, ranging from 0.9 ‰ (0.8–1.3 ‰, November and January) to 2.4 ‰ (2.2–2.6 ‰, June) and from 1.0 ‰ (0.9–1.2 ‰, November) to 2.4 ‰ (2.3–2.6 ‰, June-July) at Dome C and DDU, respectively. The modeled seasonality results from changes in the relative fractions of sulfate formed via different processes, F_i in Eq. (5) (Figure 2e, f; Table 1). During austral summer at Dome C, the relative fractions of sulfate formed by OH (F_{SO2+OH}) and H_2O_2 ($F_{S(IV)+H2O2}$) increase to 34% and 49%, respectively (Table 1), because solar radiation induces production of these oxidants. In contrast, the $F_{S(IV)+O3}$ increases to 31% during winter, when production of OH and H_2O_2 is diminished. Since S(IV) + O_3 is the only sulfate-formation pathway that leads to $\Delta^{17}O(SO_4^{2-})_{nss} > 1$ ‰, the modeled $\Delta^{17}O(SO_4^{2-})_{nss}$ values (> 2 ‰ in winter) mainly reflect the change in the relative importance of this pathway. The sulfate formed via S(IV) + HOBr ($F_{S(IV)+HOBr}$), which has $\Delta^{17}O(SO_4^{2-}) = 0$ ‰, also increases to 33% during winter, limiting the increase of $\Delta^{17}O(SO_4^{2-})_{nss}$ in the model. Although similar seasonal trends for sulfate formation pathways are found for DDU (Fig. 2f), F_{SO2+OH} is significantly higher at Dome C (34% in summer) than DDU (16% in summer) (Table 1). This is because the model prohibits aqueous-phase sulfate production at temperatures lower than –15°C and therefore most sulfate formation along with the transport of precursors towards inland Antarctica occurs through gas-phase SO_2 + OH pathway.

As a result of these estimates in sulfate formation pathways, the model roughly reproduces the observed seasonality and magnitude of $\Delta^{17}O(SO_4^{2-})_{nss}$ (Fig. 2c, d). However, the model largely underestimates observed $\Delta^{17}O(SO_4^{2-})_{nss}$ from August to December at Dome C by 0.5 to 1.1 ‰ (Fig. 2c), partially overlapping the period when the significantly positive $\Delta_{DC–DDU}$ values were observed in October to December. This underestimate implies that the model might lack sulfate formation processes that causes $\Delta^{17}O(SO_4^{2-})_{nss}$ of higher than 2.0 ± 0.3 ‰ at the inland site (Table 1) and thus the positive $\Delta_{DC–DDU}$ in this time period. Meanwhile for DDU, the model also underestimates $\Delta^{17}O(SO_4^{2-})_{nss}$ from September to October by 0.6 to 0.8 ‰, but rather slightly overestimates in January by 0.5 ‰ (Fig. 2d). This result is further discussed in the following sections within the focus of the observed inter-site differences.

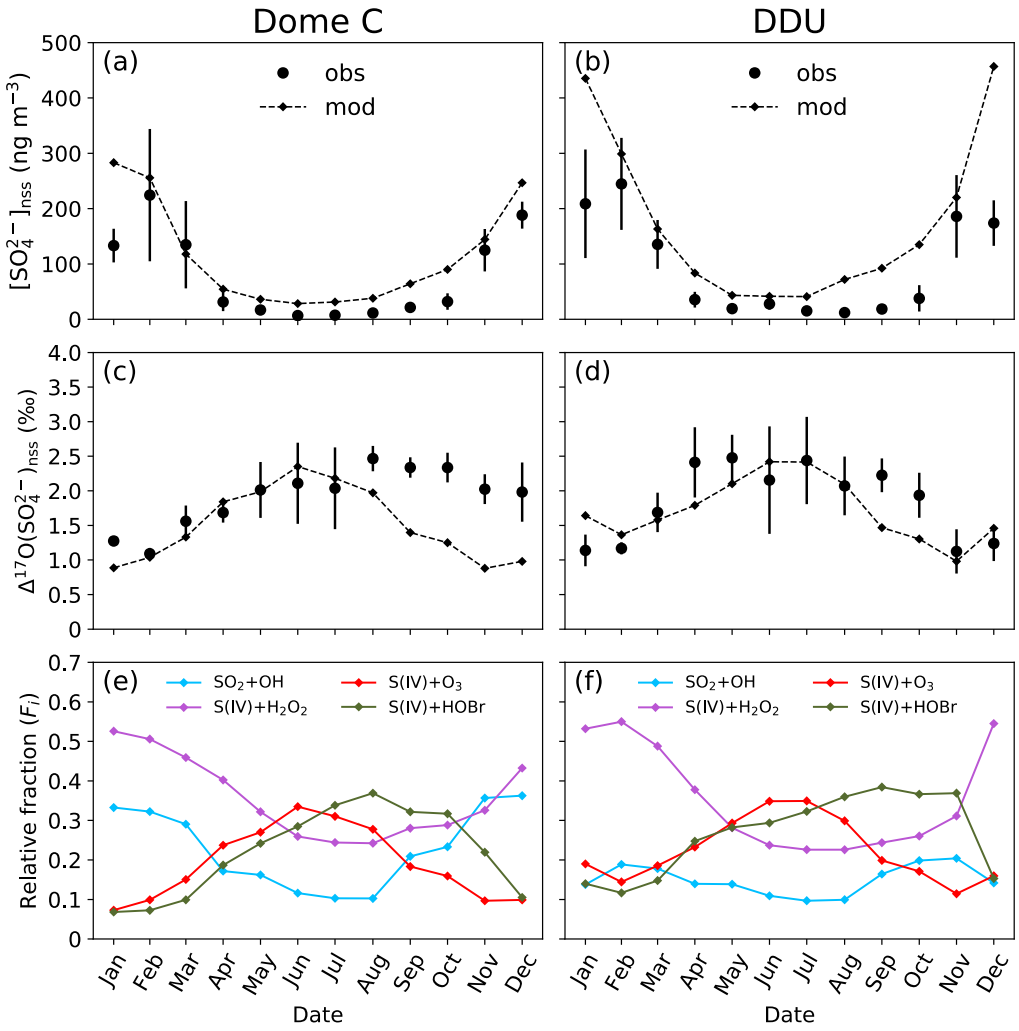

Figure 2. Comparison of observed and modeled values of (**a, b**) non-sea-salt sulfate concentration and (**c, d**) $\Delta^{17}O(SO_4^{2-})_{nss}$, and (**e, f**) calculated relative fraction of sulfate produced via different formation pathways (F_i, see Section 2.4), in the model. Left and right columns show results for Dome C and DDU, respectively.

Table 1. Model calculation of relative fraction of sulfate produced via different formation pathways and $\Delta^{17}O(SO_4^{2-})_{nss}$ values in each season in comparison to the observed $\Delta^{17}O(SO_4^{2-})_{nss}$ values (seasonal mean).

Site	Period	Observation		Model				
		Number	$\Delta^{17}O(SO_4^{2-})_{nss}$(‰)	$\Delta^{17}O(SO_4^{2-})_{nss}$(‰) [b]	F_{SO2+OH}	$F_{S(IV)+H2O2}$	$F_{S(IV)+O3}$	$F_{S(IV)+HOBr}$
Dome C	Annual	37	2.0 ± 0.5 (1.7 ± 0.1)[a]	1.5 (1.4-1.8)	0.23	0.34	0.18	0.25
	DJF	8	1.5 ± 0.5	1.0 (0.8-1.4)	0.34	0.46	0.07	0.12
	MAM	9	1.8 ± 0.3	1.7 (1.6-2.0)	0.21	0.38	0.21	0.20
	JJA	8	2.2 ± 0.5	2.2 (2.0-2.4)	0.11	0.24	0.29	0.36
	SON	12	2.2 ± 0.2	1.2 (1.1-1.5)	0.27	0.26	0.13	0.34
	OND	9	2.0 ± 0.3	1.0 (0.9-1.4)	0.32	0.32	0.11	0.26
DDU	Annual	46	1.8 ± 0.7 (1.4 ± 0.1)[a]	1.7 (1.6-2.0)	0.15	0.34	0.21	0.29
	DJF	13	1.2 ± 0.2	1.5 (1.3-1.8)	0.16	0.52	0.13	0.18
	MAM	12	2.2 ± 0.5	1.8 (1.7-2.1)	0.15	0.37	0.23	0.24
	JJA	10	2.2 ± 0.8	2.3 (2.2-2.5)	0.10	0.22	0.32	0.34
	SON	11	1.8 ± 0.6	1.3 (1.2-1.5)	0.19	0.25	0.15	0.41
	OND	9	1.3 ± 0.3	1.3 (1.1-1.5)	0.18	0.35	0.13	0.34

Note. [a] Mass-weighted average. [b] Values shown in parenthesis are possible ranges in case taking variabilities in $\Delta^{17}O$ of oxidants into account (see Section 2.4).

4 Discussion

The Δ_{DC-DDU} values different from 0 ‰ during the austral spring to summer (October–December) and during the austral autumn (March–May) (Fig. 1d) suggest that some fractions of sulfate existing at these inland and coastal sites experienced different oxidation processes. The possible processes may include long-range transport of sulfate produced above the other continents or in the stratosphere (i.e., nmb-SO_4^{2-}), in addition to DMS-sourced sulfate produced within the troposphere above the Antarctic continents and the Southern Ocean. In the former case, it is expected that $\delta^{34}S_{nss}$ values in the same aerosol samples would specifically decrease during the corresponding periods, since nmb-SO_4^{2-} has lower $\delta^{34}S_{nss}$ values than DMS-sourced sulfate (Patris et al., 2000; Pruett et al., 2004; Ishino et al., 2019). Indeed, Ishino et al. (2019) found an unexpected decrease of $\delta^{34}S_{nss}$ at Dome C in November, suggesting a significant input

of nmb-SO_4^{2-}, which is likely attributed to long-range transport of continental submicron aerosols based on a significant correlation with ^{210}Pb tracer. This input of nmb-SO_4^{2-} in November overlaps the period of the positive Δ_{DC-DDU} values. However, there were not significant correlations observed for the Δ_{DC-DDU} compared to $\delta^{34}S_{nss}$ (p = 0.39) and ^{210}Pb (p = 0.15) at Dome C (Fig. 3a, 3b, and Table S1). Therefore, this nmb-SO_4^{2-} is not likely the main factor causing the positive Δ_{DC-DDU}, while it may dilute or perturb the high $\Delta^{17}O(SO_4^{2-})_{nss}$ signature in that period. Since $\delta^{34}S_{nss}$ values were homogeneous between Dome C and DDU for the rest period of the year (Ishino et al., 2019), the negative Δ_{DC-DDU} values during the autumn would neither be associated with the contribution of nmb-SO_4^{2-}. Additionally, whereas the deposition of polar stratospheric clouds (PSCs) is thought to be a potential source of tropospheric sulfate in Antarctica, it is likely to occur during mid-winter (July–August) (Savarino et al., 2007), not coinciding with the positive and negative Δ_{DC-DDU} values. Furthermore, the relative abundance of ^{35}S, a radioactive tracer often used as a indicator of stratospheric sulfate, relative to total sulfate is maximized in June (Hill-Falkenthal et al., 2013). Therefore, the intrusion of stratospheric sulfate is not the likely reason for the Δ_{DC-DDU} values discussed here. Thus, below we discuss possible influences of regional characteristic chemistry taking place at the scale of the Antarctic continent on $\Delta^{17}O(SO_4^{2-})_{nss}$ during these periods.

4.1 Positive Δ_{DC-DDU} values in austral spring to summer

Positive Δ_{DC-DDU} in spring–summer coincides with a $[O_3]$ increase from 25 ppb to 34 ppb at Dome C (Fig. 1e) and a significant drop of $[MS^-]/[SO_4^{2-}]_{nss}$ ratios at Dome C (Fig. 1f) from 0.13 ± 0.04 (October) to 0.05 ± 0.02 (January). $[MS^-]/[SO_4^{2-}]_{nss}$ generally shows a bimodal seasonal cycle with slight increase from winter (July-August; 0.06 ± 0.01) to spring (October; 0.13 ± 0.04), followed by a significant drop in summer (January; 0.05 ± 0.02) and then increases to maximum values in autumn (March; 0.25 ± 0.09) at Dome C (Legrand et al., 2017b). Legrand et al. (2017b) found that the decline of $[MS^-]/[SO_4^{2-}]_{nss}$ during summer coincides with periods of high photochemical activity as indicated by high O_3 levels, suggesting the occurrence of chemical destruction of MS^-. Legrand et al. (2017b) also showed that the decrease in $[MS^-]/[SO_4^{2-}]_{nss}$ at DDU is less significant than Dome C, while MS^- destruction may also occur at DDU where is frequently exposed to the highly oxidative atmosphere from the interior Antarctica during summer due to katabatic wind (Legrand et al., 2016a). The co-occurrence of MS^- destruction at Dome C and positive Δ_{DC-DDU} (Fig. 1d and 1f) is striking, suggesting the possibility that MS^- destruction produces sulfate with significantly high $\Delta^{17}O(SO_4^{2-})_{nss}$ at Dome C and leads to the high Δ_{DC-DDU}. This possibility is supported by the negative co-variation between the Δ_{DC-DDU} and $[MS^-]/[SO_4^{2-}]_{nss}$ at Dome C for October to December with p value of 0.01 (Fig. 3c and Table S1), where Δ_{DC-DDU} tends to be higher as $[MS^-]/[SO_4^{2-}]_{nss}$ becomes lower.

This hypothesis requires that MS^- possesses significantly high $\Delta^{17}O$ signature or MS^- destruction occurs via its oxidation by O_3 to produce sulfate. It is known that MS^- formation in the marine boundary layer involves O_3 as well as BrO, which is produced via Br + O_3 (Zhang et al., 1997), as important oxidants (von Glasow and Crutzen, 2004; Hoffmann et al., 2016). These oxidants would imprint a high $\Delta^{17}O$ value on MS^-. To date, however, there are no observations or estimates of $\Delta^{17}O(MS^-)$. The mechanism and the subsequent products of MS^- destruction in inland Antarctica remain unclear. While MS^- oxidation by OH, SO_4^-, Cl, and Cl_2^- have been

proposed so far (Zhu et al., 2003a, 2003b; Zhu, 2004), there is no evidence for a reaction with O_3. A previous box model study simulating multi-phase sulfur chemistry (Hoffmann et al., 2016) indicated that aqueous-phase oxidation of MS^- by OH to produce sulfate (Zhu et al., 2003a) is the dominant pathway under typical pristine marine boundary layer (MBL) conditions (Bräuer et al., 2013). Furthermore, it is also shown by a flow tube chamber experiment that MS^- can be oxidized on deliquesced aerosols to form sulfate, which may lead to shorter lifetime of MS^- than in condenced aqueous-phase in MBL (Mungall et al., 2018). Legrand et al. (2017b) mentioned that, although the chance of aerosol experiencing aqueous-phase chemistry is far lower than in the marine boundary layer, far more acidic conditions on the Antarctic Plateau compared to the marine boundary layer would favor the production of OH via the reaction of O_3 with O_2^- (Ervens et al., 2003). Thus, here we assume MS^- oxidation by OH in aqueous-phase or on aerosols as the mechanism for MS^- destruction, and for the first time estimate $\Delta^{17}O$ transferred from DMS oxidation to MS^- and then to sulfate.

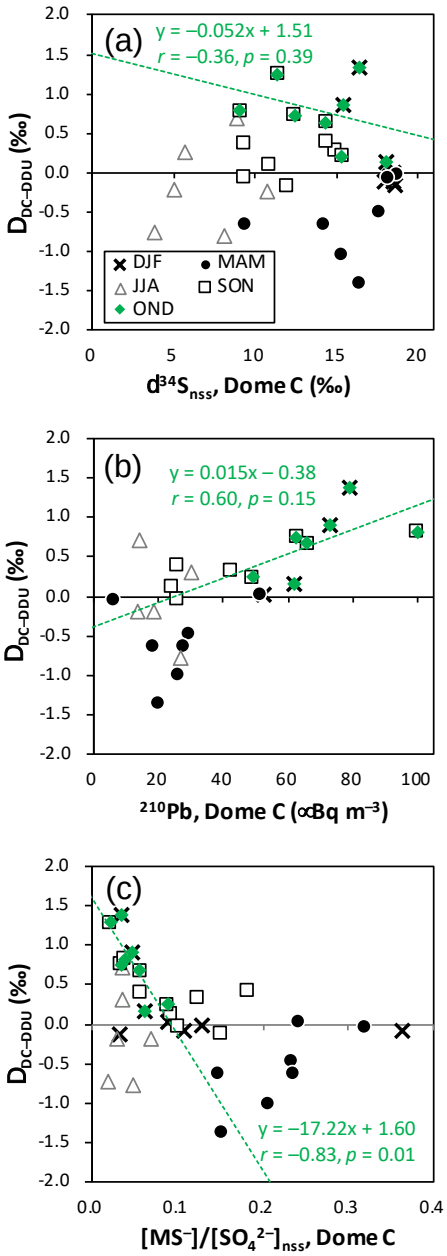

503

504 **Figure 3**. Variations of Δ_{DC-DDU} against (a) $\delta^{34}S_{nss}$, (b) ^{210}Pb, and (c) $[MS^-]/[SO_4^{2-}]_{nss}$, at Dome
505 C. Data for summer (DJF), autumn (MAM), winter (JJA), and spring (SON) are plotted with
506 crosses, circles, triangles, and squares, respectively. Data for October 29th to December 23rd
507 (OND) are plotted with green diamonds, with the linear least-squares fit shown by green dashed
508 lines.
509

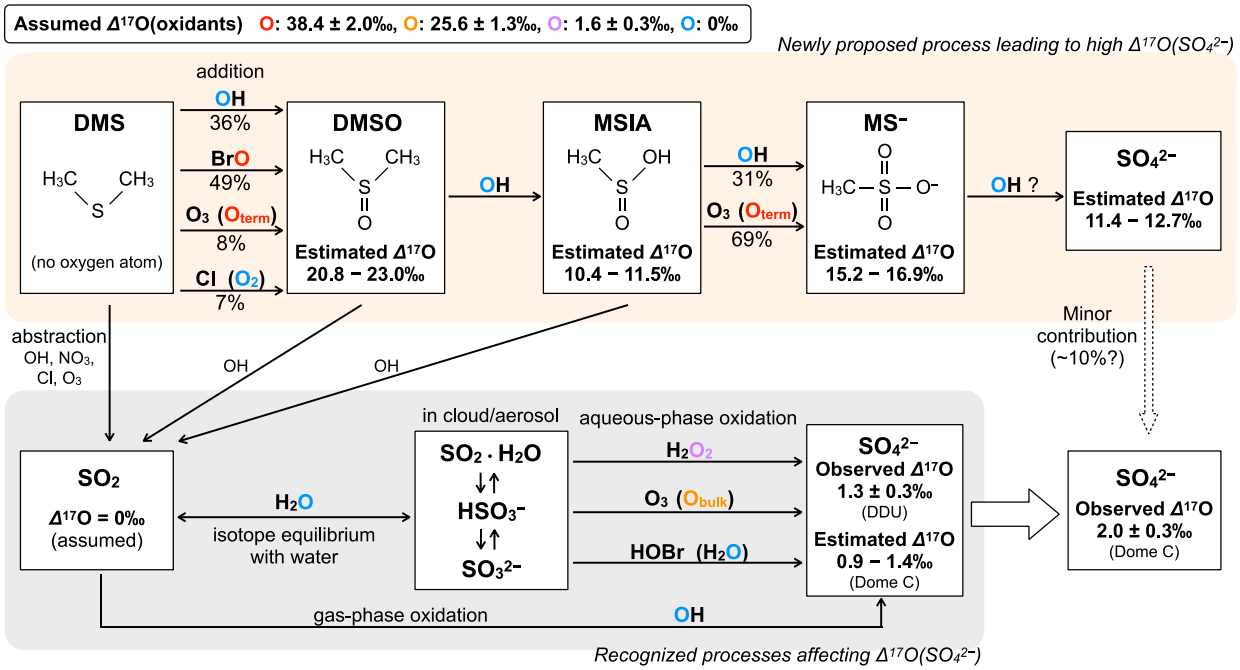

Figure 4. Schematic of sulfate formation processes affecting $\Delta^{17}O(SO_4^{2-})_{nss}$ considered in this study. The processes in upper row (orange shaded) are described in Section 4.1, whereas those in lower row (grey shaded) are described in Section 2.4. The $\Delta^{17}O$ of oxidants are indicated by different colors. The $\Delta^{17}O$ of sulfur species shown in the figure represent the mean values for October to December. The percentages shown under arrows are the relative contributions of each pathway averaged within the troposphere in 60–90°S during October to December, which are estimated by the model with detailed DMS chemistry by Chen et al. (2018).

Table 2. Expected $\Delta^{17}O$ values of sulfur species produced through oxidation of DMS from different reaction mechanisms.

Reaction	$\Delta^{17}O(X)_j$	Reference
DMS + OH (add)	$\Delta^{17}O(DMSO)_{DMS+OH} = \Delta^{17}O(OH)$	Barnes et al. (2006)
DMS + BrO	$\Delta^{17}O(DMSO)_{DMS+BrO} = \Delta^{17}O(BrO) = \Delta^{17}O(O_3)_{term}$	Ingham et al. (1999)
DMS + O_3	$\Delta^{17}O(DMSO)_{DMS+O3} = \Delta^{17}O(O_3)_{term}$	Gershenzon et al. (2001)
DMS + Cl (+ O_2)	$\Delta^{17}O(DMSO)_{DMS+Cl} = \Delta^{17}O(O_2)$	Barnes et al. (2006)
DMSO + OH	$\Delta^{17}O(MSIA)_{DMSO+OH} = 1/2\ \Delta^{17}O(DMSO) + 1/2\ \Delta^{17}O(OH)$	Wang and Zhang (2002)
MSIA + OH	$\Delta^{17}O(MS^-)_{MSIA+OH} = 2/3\ \Delta^{17}O(MSIA) + 1/3\ \Delta^{17}O(OH)$	Gonzalez-Garcia et al. (2007); Tian et al. (2007)
MSIA + O_3	$\Delta^{17}O(MS^-)_{MSIA+O3} = 2/3\ \Delta^{17}O(MSIA) + 1/3\ \Delta^{17}O(O_3)_{term}$	Flyunt et al. (2001); Kukui et al. (2000)
MS^- + OH	$\Delta^{17}O(SO_4^{2-})_{MS+OH} = 3/4\ \Delta^{17}O(MS^-) + 1/4\ \Delta^{17}O(OH)$	Zhu et al., (2003a); Hoffmann et al. (2016)

Figure 4 summarizes the hypothesized sulfate formation processes via MS^- oxidation possibly transferring high $\Delta^{17}O$ to sulfate, in addition to the recognized processes explained in Section 2.4. The reaction scheme includes DMS oxidation into dimethyl sulfoxide (DMSO; $CH_3S(O)CH_3$), methyl sulfinic acid (MSIA; $CH_3S(O)OH$), and then to MS^-, as well as production of SO_2 from each species, whose importance in the marine boundary layer are recognized (Barnes et al., 2006; von Glasow and Crutzen, 2004; Hoffmann et al., 2016; Chen et al., 2018). Note that gas-phase and aqueous-phase reactions using the same oxidants are considered as one pathway for simplification, since they will result in the same $\Delta^{17}O(SO_4^{2-})$. We also summarize the formula for calculating the $\Delta^{17}O$ value of each sulfur species X (DMSO, MSIA, MS^-, and SO_4^{2-}) produced by each reaction j ($\Delta^{17}O(X)_j$) in Table 2, which is determined based on mechanisms of respective oxidation pathways as follows.

At the first step, DMS oxidation into DMSO includes four different oxidation pathways reacting with OH, BrO, O_3, and Cl. These reactions generally occur through adduct of the oxidant to the sulfur atom of DMS (Barnes et al., 2006; Ingham et al. 1999; Gershenzon et al., 2001), transferring oxygen atoms of oxidants to the produced DMSO. Therefore, the $\Delta^{17}O$ transferred to DMSO via DMS + OH, DMS + BrO, and DMS + O_3 reflect $\Delta^{17}O$ values of each oxidant. $\Delta^{17}O$ of DMSO produced via DMS + OH is assumed to be equal to $\Delta^{17}O$ of OH, i.e., 0 ‰. Since ^{17}O excess is located at the two terminal O atoms of O_3 (O_3-terminal) (Bhattacharya et al., 2008; Janssen and Tuzson, 2006), $\Delta^{17}O(O_3)_{term}$ is assumed to be 38.4 ± 2.0 ‰ (= 3/2 × $\Delta^{17}O(O_3)_{bulk}$). In addition, BrO receives O_3-terminal via Br + O_3 (Zhang et al., 1997). DMS + O_3 and DMS + BrO are thus expected to produce DMSO with $\Delta^{17}O$ of 39 ‰. Since DMS + Cl pathway is expected to form $CH_3S(Cl)CH_3$, which is followed by subsequent oxidation by O_2 (Barnes et al., 2006), $\Delta^{17}O_{DMS+Cl}$ is assumed to be equal to $\Delta^{17}O(O_2)$ (= –0.3 ‰; Barkan and Luz, 2005). During DMSO oxidation by OH into MSIA, one of the two oxygen atoms of produced MSIA is from DMSO while another comes from OH (Bardouki et al., 2002), suggesting that $\Delta^{17}O(MSIA)_{DMSO+OH}$ is determined as the sum of 1/2 $\Delta^{17}O$(DMSO) and 1/2 $\Delta^{17}O$(OH). MSIA is oxidized into MS^- by OH or O_3. In MSIA + OH, O-atom added to MS^- is assumed to come from OH, since OH is added to S-atom of MSIA to form $CH_3S(O)(OH)_2$ adduct before its reaction with O_2 to form MS^- (Bardouki et al., 2002). In MSIA + O_3, it is experimentally indicated that O_3-terminal transfers to MS^- (Flyunt et al., 2001). In both reactions, two of three O-atoms of MS^- are preserved from MSIA. Therefore, $\Delta^{17}O$ transferring to MS^- via each reaction is determined as sum of 2/3 $\Delta^{17}O$(MSIA) and 1/3 $\Delta^{17}O$(oxidant). Finally, assuming MS^- + OH provides one O-atom from OH to produce sulfate, $\Delta^{17}O(MS^-)_{MS+OH}$ is determined as the sum of 3/4 $\Delta^{17}O(MS^-)$ and 1/4 $\Delta^{17}O$(OH) (Table 2).

With the above assumptions on $\Delta^{17}O$ transferring processes, $\Delta^{17}O$ value of species X is determined by the isotopic mass balance as the following equation:

$$\Delta^{17}O(X) = \sum \Delta^{17}O(X)_j \, f_j \quad , \tag{6}$$

$$f_j = P(X)_j / \sum P(X)_j \quad , \tag{7}$$

where f_j is relative contribution of reaction j for production of X ($P(X)$). To obtain $\Delta^{17}O(MS^-)$, we here used $P(X)_j$ and thus f_j estimated by the previous simulation using GEOS-Chem by Chen et al. (2018), which incorporated whole sulfur chemistry shown in Figure 4. We used the mean $P(X)_j$ within the troposphere in 60–90°S during October to December. For production of DMSO,

f_{DMS+OH}, $f_{DMS+BrO}$, f_{DMS+O3}, and f_{DMS+Cl} are estimated to be 36%, 49%, 8%, and 7%, respectively. By applying these estimated f_j with $\Delta^{17}O(X)_j$ defined in Table 2 and Eq. (6), the $\Delta^{17}O(DMSO)$ is estimated to be 20.8–23.0 ‰. Since MSIA production occurs via DMSO + OH only ($f_{DMSO+OH}$ = 100%), $\Delta^{17}O(MSIA)$ is equivalent to $\Delta^{17}O(MSIA)_{DMSO+OH}$ = 10.4–11.5 ‰. For production of MS^-, $f_{MSIA+OH}$ and $f_{MSIA+O3}$ are estimated to be 31% and 69%, respectively, consequently leading to $\Delta^{17}O(MS^-)$ of 15.2–16.9 ‰. Finally, $\Delta^{17}O(SO_4^{2-})$ derived via MS^- destruction, $\Delta^{17}O_{MS+OH}$, is estimated to be 11.4–12.7 ‰.

If the oxidation of MS^- into sulfate fully corresponds to the difference in $[MS^-]/[SO_4^{2-}]_{nss}$ of 0.09 between Dome C (0.05 ± 0.02) and DDU (0.14 ± 0.07) during October to December, $\Delta^{17}O(SO_4^{2-})_{nss}$ can increase by 1.1 ‰ (= $\Delta^{17}O(SO_4^{2-})_{MS+OH} \times 0.09$), which is close to the observed Δ_{DC-DDU} of ca. 0.7 ‰. Additionally, the intercept of the slope of Δ_{DC-DDU} versus $[MS^-]/[SO_4^{2-}]_{nss}$ relationship (Fig. 3) suggests that $\Delta^{17}O(SO_4^{2-})_{nss}$ can increase by 1.6 ‰ if all MS^- observed at DDU was converted to sulfate at Dome C (i.e., $[MS^-]/[SO_4^{2-}]_{nss}$ decreases from 0.14 ± 0.07 to 0), which is consistent with $\Delta^{17}O(SO_4^{2-})_{MS+OH} \times 0.14 \pm 0.07 = 1.7 \pm 0.9$ ‰. These consistencies imply that the positive Δ_{DC-DDU} observed in the austral spring–summer is mainly caused by MS^- destruction. We therefore conclude that MS^- destruction and subsequent sulfate production along with transport over the Antarctic Plateau is the most likely process responsible for the positive Δ_{DC-DDU} in the austral spring–summer at inland Antarctica.

The model underestimate of $\Delta^{17}O(SO_4^{2-})_{nss}$ for Dome C during August to December by 0.5–1.1 ‰ (Fig. 2c) are also within the possible range of the expected shift in $\Delta^{17}O(SO_4^{2-})_{nss}$ by MS^- destruction, i.e., 1.6‰ at maximum (Fig. 3). Note that the MS^- destruction becomes significant from November (Fig. 1f), only for the latter period of this underestimate of $\Delta^{17}O(SO_4^{2-})_{nss}$ in the model. Additionally, the model also underestimates $\Delta^{17}O(SO_4^{2-})_{nss}$ for DDU during September to October by 0.6–0.8 ‰, while does not during November to December. The absense of $\Delta^{17}O(SO_4^{2-})_{nss}$ underestimate for DDU during November-December is expected because MS^- destruction in the mid-summer is less significant at DDU than Dome C (Legrand et al., 2017b). On the other hand, the underestimates of $\Delta^{17}O(SO_4^{2-})_{nss}$ in early spring at both sites indicate the other missing processes such that impacts both sites. One idea that might cause the underestimates of $\Delta^{17}O(SO_4^{2-})_{nss}$ is the underestimates of $F_{S(IV)+O3}$ due to the excessive sulfur loading (Fig. 2a and 2b). Since S(IV) + O_3 reaction prefers higher pH condition, the excessive acidification of cloud water and sea-salt aerosols induced by the overestimates of $[SO_4^{2-}]_{nss}$ may result in surpression of S(IV) + O_3. This idea is uncertain because the overestimate of $[SO_4^{2-}]_{nss}$ is not specific for early spring but seen for year-round. Additionally, there remains possibility that $\Delta^{17}O(OH)$ is higher than 3 ‰ (Savarino et al., 2016), that might partially correspond to the underestimates in $\Delta^{17}O(SO_4^{2-})_{nss}$. Future modeling work incorporating DMSO, MSIA, MS^-, and sulfate possessing different $\Delta^{17}O$ signatures is necessary to examine if this underestimate in $\Delta^{17}O(SO_4^{2-})_{nss}$ at Dome C corresponds to the lack of MS^- destruction in the model.

This finding that confirms the suspected occurrence of an efficient atmospheric oxidation of MS^- into sulfate over the Antarctic plateau has an important implication for the interpretation of ice-core $\Delta^{17}O(SO_4^{2-})_{nss}$ records. Previous studies revealed that, in Antarctica, MS^- in snow is largely lost after deposition (Wagnon et al., 1999; Delmas et al., 2003; Weller et al., 2004). While the mechanism of this MS^- loss in snow is under debated, there are two proposed ideas: physical migration of MS^- within firn layers and possibly by MS^- oxidation by OH in quasi-brine layer of snow grain. If being viable, the latter MS^- oxidation should increase $\Delta^{17}O(SO_4^{2-})_{nss}$

values in snow after deposition of MS^- and sulfate. Indeed, the previous measurements of $\Delta^{17}O(SO_4^{2-})_{nss}$ in Antarctic ice corresponding to the present-day warm climate period (Holocene) average 2.8 ± 0.4 ‰ (Alexander et al., 2002, 2003; Kunasek et al., 2010; Sofen et al., 2014), which is significantly higher than the annual mass-weighted average of $\Delta^{17}O(SO_4^{2-})_{nss}$ of 1.7 ± 0.1 ‰ in aerosols at Dome C (Table 1). Even the maximum monthly mean $\Delta^{17}O(SO_4^{2-})_{nss}$ of 2.5 ± 0.1 ‰ in July cannot reach the ice-core $\Delta^{17}O(SO_4^{2-})_{nss}$ of 2.8 ± 0.4 ‰, indicating the additional sulfate production with the higher $\Delta^{17}O(SO_4^{2-})_{nss}$ in snow after deposition. The degree of post-depositional loss of MS^- tends to be higher at sites with lower snow accumulation rates (Delmas et al., 2003), and reaches 80–90% at Vostok where the present-day snow accumulation rate is 2.2 g cm^{-2} yr^{-1} (Wagnon et al., 1999). Assuming 90% of MS^- in snow is converted into sulfate at Dome C where the accumulation rate (2.7 g cm^{-2} yr^{-1}) is similar to the one in Vostok, combined with the annual mean $[MS^-]/[SO_4^{2-}]_{nss}$ in aerosols of 0.11 (Legrand et al., 2017b), $\Delta^{17}O(SO_4^{2-})_{nss}$ can increase by 1.1–1.3 ‰ (= $\Delta^{17}O(SO_4^{2-})_{MS+OH} \times 0.11 \times 0.9$) at maximum. This estimated post-depositional shift in $\Delta^{17}O(SO_4^{2-})_{nss}$ is in agreement with the difference between atmosphere and snow $\Delta^{17}O(SO_4^{2-})_{nss}$, indicating the significance of the post-depositional oxidation of MS^- to sulfate as a controlling factor of ice-core $\Delta^{17}O(SO_4^{2-})_{nss}$. Thus, we argue that, to use ice-core $\Delta^{17}O(SO_4^{2-})_{nss}$ for assessing past atmospheric oxidant chemistry, it is necessary to correct the ice-core $\Delta^{17}O(SO_4^{2-})_{nss}$ for this process. For this purpose, the investigation of the relationship between $\Delta^{17}O(SO_4^{2-})_{nss}$ and $[MS^-]/[SO_4^{2-}]_{nss}$ in snow at various sites with different snow accumulation rates over Antarctica will be required as a future step. Additionally, observations of $\Delta^{17}O(MS^-)$ in aerosols, snow, and ice will provide useful information to prove the proposed mechanisms as well as to constrain the sulfur chemistry in atmospheric chemical transport models.

4.2 Negative $\Delta_{DC–DDU}$ values in austral autumn

The negative $\Delta_{DC–DDU}$ values ranging –1.4 ± 0.6 ‰ to –0.5 ± 0.3 ‰ were observed in austral autumn (March to May) (Fig. 1d), suggesting that sulfate with higher $\Delta^{17}O(SO_4^{2-})_{nss}$ is produced at or transported to DDU, compared to Dome C. The largest negative $\Delta_{DC–DDU}$ value of –1.4 ± 0.6 ‰ was observed in April. Meanwhile, the model in the present study slightly underestimates the observed $\Delta^{17}O(SO_4^{2-})_{nss}$ at DDU in April (modeled: 1.6–2.1 ‰, observed: 2.4 ± 0.5 ‰), but reproduces the observed $\Delta^{17}O(SO_4^{2-})_{nss}$ at Dome C (modeled: 1.7–2.1 ‰, observed: 1.7 ± 0.1 ‰) within the range of standard deviation of observations (Fig. 2). Below we consider processes that possibly lead to high $\Delta^{17}O(SO_4^{2-})_{nss}$ at DDU in this period and that also can explain the underestimate of $\Delta^{17}O(SO_4^{2-})_{nss}$ at DDU in the model.

The negative $\Delta_{DC–DDU}$ values in March to May coincide with the period when $[Br_y^*]$ is minimal at both sites (Fig. 1g). This $[Br_y^*]$ minimum in autumn is thought to be a result of the decrease in Br_y emission from sea-salt provided from both open ocean and sea-ice related process (Legrand et al., 2016b). Since Br_y^* includes HOBr that reacts with S(IV) to produce sulfate with $\Delta^{17}O(SO_4^{2-}) = 0$ ‰ as mentioned in Section 2.4, the decrease in $[Br_y^*]$ may cause the reduction of $F_{S(IV)+HOBr}$ and the increase in $\Delta^{17}O(SO_4^{2-})_{nss}$. Since Br_y^* emission sources are close to coastal regions, the decrease of $[Br_y^*]$ during autumn compared to the other period is larger at DDU (4.7 ± 1.7 ng m^{-3} for MAM compared to 8.9 ± 1.8 ng m^{-3} for JJA) than Dome C (1.0 ± 0.4 ng m^{-3} for MAM compared to 1.9 ± 0.8 ng m^{-3} for JJA). Given the larger decrease of $[Br_y^*]$ at

DDU than Dome C during autumn, it seems that $F_{S(IV)+HOBr}$ might decrease and $\Delta^{17}O(SO_4^{2-})_{nss}$ might increase at larger degree at DDU than Dome C, resulting in the negative Δ_{DC-DDU} values. However, although the model also shows the larger decrease in $[Br_y^*]$ during autumn at DDU (3.5 ± 1.4 ng m^{-3} for MAM compared to 12.8 ± 2.7 ng m^{-3} for JJA) than Dome C (5.1 ± 1.4 ng m^{-3} for MAM compared to 2.2 ± 0.5 ng m^{-3} for JJA) (Fig. S1), the change in the modeled $F_{S(IV)+HOBr}$ were smaller at DDU (23% for MAM compared to 33% for JJA) than Dome C (18% for MAM compared to 33% for JJA) (Table 1). Therefore, the larger decrease in $[Br_y^*]$ at DDU than Dome C does not lead to a larger decrease in $F_{S(IV)+HOBr}$ at DDU in the model. Furthermore, despite the good reproducibility of $[Br_y^*]$ at DDU during MAM by the model (observed: 4.7 ± 1.7 ng m^{-3}, modeled: 3.5 ± 1.4 ng m^{-3}), the model tends to underestimate tropospheric BrO vertical column density in 60 to 90°S during March to April by a factor of ~4 (Fig. S2), implying that the model could also underestimate HOBr abundance. The underestimate of HOBr abundance would lead to underestimate of $F_{S(IV)+HOBr}$ and overestimate of $\Delta^{17}O(SO_4^{2-})_{nss}$, which is opposed to the obtained result of underestimate in $\Delta^{17}O(SO_4^{2-})_{nss}$ during autumn at DDU. Rather, given that BrO in 60 to 90°S is underestimated year-round (Fig. S2), it could be a reason for overestimate of $\Delta^{17}O(SO_4^{2-})_{nss}$ such that seen for DDU in January (Fig. 2d). We note that, based on the kinetics of HSO_3^- + HOCl investigated by a flow tube experiment, Liu and Abbatt (2020) recently determined reaction rate constant of HSO_3^- + HOBr ($k_{HOBr+HSO3-}$) which was estimated to be two orders of magnitude lower than the values used in atmospheric models including GEOS-Chem. However, Chen et al. (2017) had performed a sensitivity test with the two orders of magnitude lower $k_{HOBr+HSO3-}$ and showed that the contribution of S(IV) + HOBr reaction to the global sulfate formation does not change because this reaction is limited by gas diffusion of HOBr into cloud droplets. Thus, it seems that the current understanding in S(IV)+HOBr pathway and related reactive bromine chemistry cannot explain the underestimate of $\Delta^{17}O(SO_4^{2-})_{nss}$ at DDU during the autumn in the model.

Another possible explanation is the increase in $\Delta^{17}O(SO_4^{2-})_{nss}$ at DDU associated with the aqueous-phase S(IV) + O_3 pathway in sea-salt aerosol. As mentioned in Section 2.3, fresh sea-salts typically contain alkaline solution (pH ~ 8) where the S(IV) + O_3 pathway is efficient prior to aerosol acidification (Alexander et al., 2005). It is thus expected that, while sea-salt loading in autumn (0.9 ± 0.4 μg m^{-3} for MAM) is lower than in summer (1.1 ± 0.4 μg m^{-3} for DJF) by only a factor of 1.2, the $[SO_4^{2-}]_{nss}$ level in autumn (57 ± 46 ng m^{-3}) is a factor of 4 lower than that in summer (215 ± 79 ng m^{-3}), leading to slower sea-salt acidification, possibly allowing S(IV) + O_3 to proceed. This possibility seems to be supported by the negative covariation between the Δ_{DC-DDU} and $[SO_4^{2-}]_{ss}/[SO_4^{2-}]_{total}$ at DDU, an assumed index of the degree of sea-salt acidification, for the data during March to May with $r = -0.96$ and $p < 0.01$ (Fig. 5 and Table S1), where the Δ_{DC-DDU} tends to be lower as $[SO_4^{2-}]_{ss}/[SO_4^{2-}]_{total}$ becomes higher. Note that, however, since both $\Delta^{17}O(SO_4^{2-})_{nss}$ and $[SO_4^{2-}]_{ss}/[SO_4^{2-}]_{total}$ are determined as functions of $k \times [Na^+]$ in Eq. (1), the correlation between the Δ_{DC-DDU} and $[SO_4^{2-}]_{ss}/[SO_4^{2-}]_{total}$ could be an artefact of the calculation. If we assume $[Na^+]/[SO_4^{2-}]_{total}$ as an index of sea-salt loading relative to titrating acids without using k value, the correlation coefficient compared to Δ_{DC-DDU} becomes less significant ($r = -0.74$ and $p = 0.06$; Table S1). Hence, it is currently difficult to conclude the role of sea-salt controlling $\Delta^{17}O(SO_4^{2-})_{nss}$ and Δ_{DC-DDU} values based on the available data. In the meantime, the sea-salt aerosol in the model may be acidified excessively because of the overestimate of $[SO_4^{2-}]_{nss}$ (Fig. 2a and 2b), while the model fairly reproduces the abundances of sea-salt aerosols at DDU by implementing sea-salts production from blowing snow sublimation (Huang and Jaeglé, 2017; Fig. S1). The excessive acidification of sea-salt in the model would

lead to the underestimate of $F_{S(IV)+O3}$ and then $\Delta^{17}O(SO_4^{2-})_{nss}$. Therefore, the small underestimate of $\Delta^{17}O(SO_4^{2-})_{nss}$ at DDU during autumn might be partly compensated by correcting $[SO_4^{2-}]_{nss}$.

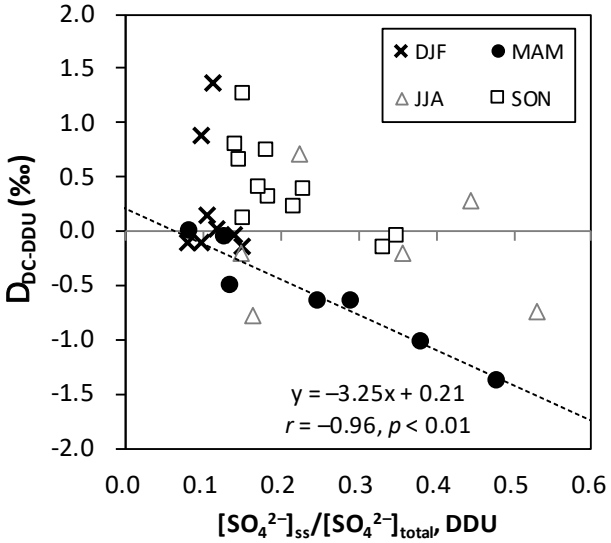

Figure 5. Relationship between $[SO_4^{2-}]_{ss}/[SO_4^{2-}]_{total}$ at DDU and $\Delta_{DC\text{-}DDU}$. Symbols for different seasons are same as Fig. 3. The dashed line shows the linear least-squares fit for autumn (MAM).

In both cases, to obtain the negative Δ_{DC-DDU} values, sulfate with high $\Delta^{17}O(SO_4^{2-})_{nss}$ of 1.9 ± 0.2 ‰ during autumn at DDU needs to be reduced and sulfate with lower $\Delta^{17}O(SO_4^{2-})_{nss}$ needs to be increased along with the transport of sulfate and its precursors towards inland Antarctica. It is reasonable that, since liquid water content becomes zero at –40°C (Jeffery and Austin, 1997; Pruppacher, 1995), aqueous-phase S(IV) oxidation is strictly limited and sulfate produced via gas-phase SO_2 + OH pathway with $\Delta^{17}O(SO_4^{2-})_{nss}$ = 0 ‰ is more important at inland Antarctica, represented by Dome C where the annual mean temperature is –50°C (Argentini et al., 2014). Additionally, given that $[Na^+]$ is two orders of magnitude lower at Dome C (ca. 5 ng m^{-3}; Legrand et al., 2017a) than DDU (ca. 300 ng m^{-3}; Jourdain and Legrand, 2002), it is expected that the sea-salt particles preferentially deposit during transport towards inland Antarctica together with sulfate produced in sea-salt, possibly leading to sulfate with lower $\Delta^{17}O(SO_4^{2-})_{nss}$ values at Dome C. Thus, it seems qualitatively reasonable to observe lower $\Delta^{17}O(SO_4^{2-})_{nss}$ at Dome C than DDU.

Thus, the changes in sulfate formation processes responsible for the negative Δ_{DC-DDU} values during March to May are uncertain. Considering the small but significant underestimate in $\Delta^{17}O(SO_4^{2-})_{nss}$ at DDU in the model despite of the good reproducibility at Dome C in that period, we looked into the processes that would be more important around coastal regions than inland such as the decrease in $F_{S(IV)+HOBr}$ and the increase in $F_{S(IV)+O3}$ in sea-salt particles at DDU. However, both of them are not decisive. Given the larger abundances of reactive bromine at coastal regions of West Antarctica than those of East Antarctica (Theys et al., 2011; Saiz-Lopez et al., 2007; Grilli et al., 2013), further observations of $\Delta^{17}O(SO_4^{2-})_{nss}$ at different coastal sites around Antarctica would help to constrain the importance of those processes.

5 Conclusions

We investigated the consequences of characteristic oxidation chemistry in Antarctica for sulfate formation processes and $\Delta^{17}O(SO_4^{2-})_{nss}$ by comparing weekly $\Delta^{17}O(SO_4^{2-})_{nss}$ observations at inland site Dome C and those previously obtained at coastal site DDU in the same year 2011. The $\Delta^{17}O(SO_4^{2-})_{nss}$ at Dome C showed lower values in austral summer (1.1 ± 0.1 ‰ in February) and higher values in winter (2.5 ± 0.2 ‰ in August), with a mass-weighted annual average of 1.7 ± 0.1 ‰, which are generally consistent with previous observations at DDU. This seasonality in $\Delta^{17}O(SO_4^{2-})_{nss}$ at Dome C is roughly reproduced by the GEOS-Chem atmospheric chemistry transport model, reflecting the increased relative fraction of sulfate produced via SO_2 + OH (34%) and S(IV) + H_2O_2 (48%) in summer in contrast to the increased fraction of S(IV) + O_3 (30%) and S(IV) + HOBr (34%) in winter. The model also reproduces the $\Delta^{17}O(SO_4^{2-})_{nss}$ at DDU with estimated sulfate formation processes similar to Dome C but with lower fraction of gas-phase OH oxidation for DDU (16% in summer).

Aside from those general seasonal trends, we found that there are significant differences in $\Delta^{17}O(SO_4^{2-})_{nss}$ at Dome C and DDU during the austral spring–summer (October to December) and the austral autumn (March to May), indicating the contribution of specific oxidation chemistry to sulfate at each site. For spring–summer, the higher $\Delta^{17}O(SO_4^{2-})_{nss}$ at Dome C than DDU was observed, which coincides with the period when chemical MS^- destruction is enhanced under the high photochemical activity at Dome C. Combined with the first estimate of $\Delta^{17}O(MS^-)$ based on the isotopic mass balance calculations, we conclude that MS^- destruction producing sulfate with $\Delta^{17}O(SO_4^{2-})_{nss}$ as high as 12 ‰ is the most likely process responsible for the observed high $\Delta^{17}O(SO_4^{2-})_{nss}$ at Dome C, and suggests that MS^- destruction is responsible for ca. 10% of total sulfate during spring–summer at this inland Antarctic location. This finding has important implications for the interpretation of ice-core $\Delta^{17}O(SO_4^{2-})_{nss}$ records, since it is known that MS^- can be also chemically destroyed in snow. This process may lead to a significant post-depositional increase in $\Delta^{17}O(SO_4^{2-})_{nss}$ of over 1 ‰ and reconcile the existing discrepancy between the $\Delta^{17}O(SO_4^{2-})_{nss}$ in the atmosphere and ice. For a precise interpretation of ice-core $\Delta^{17}O(SO_4^{2-})_{nss}$ records, future works investigating the relationship between $\Delta^{17}O(SO_4^{2-})_{nss}$ and $[MS^-]/[SO_4^{2-}]_{nss}$ in snow at various sites over Antarctica are required to formulate the post-depositional shift of $\Delta^{17}O(SO_4^{2-})_{nss}$. Additionally, the calculation of $\Delta^{17}O(MS^-)$ should be implemented into the model that is used for simulation of the past $\Delta^{17}O(SO_4^{2-})_{nss}$. Developments of analytical methods for $\Delta^{17}O(MS^-)$ are also necessary to prove the proposed mechanisms as well as to constrain the models. Meanwhile, the higher $\Delta^{17}O(SO_4^{2-})_{nss}$ at DDU than Dome C during autumn may be associated with decreased contribution of S(IV) + HOBr due to the limited reactive bromine availability and/or the increasd contribution of S(IV) + O_3 due to the insufficient acidification of sea-salt at DDU. Further observations of $\Delta^{17}O(SO_4^{2-})_{nss}$ at various coastal sites over Anarctica will help to constrain the impact of these processes.

Conflict of Interest

The authors declare no conflicts of interest.

Data Availability Statement

Data presented in this article are available at http://dx.doi.org/10.17632/xfr8ffn9xv.1.

Acknowledgments

We thank Shuting Zhai for providing support to S.I. and S.H for handling the GEOS-Chem model. We acknowledge financial supports and field supplies for winter and summer campaigns at Dome C and DDU by the Institut Polaire Français Paul Emile Victor (IPEV) from program 1011 (SUNITEDC) and program 1177 (CAPOXI 35–75). We also thank aerosol data provided via the French Environmental Observation Service CESOA, which was supported by IPEV and the National Institute of Sciences of the Universe (INSU-CNRS). We acknowledge JSPS KAKENHI (JP17J08978 (S.I.), JP19J00682 (S.I.), JP16H05884 (S.H.), JP18H05050 (S.H.), JP20H04305 (S.H.), JP20H04969 (S.H.), and JP17H06105 (N.Y. and S.H.)) from the Ministry of Education, Culture, Sports, Science and Technology (MEXT), Japan. We acknowledge Labex OSUG@2020 (Investissements d'avenir – ANR10 LABX56), the French Agence Nationale de la Recherche (ANR) FOFAMIFS project (grant ANR—14-CE33-0009-01) and EAIIST project (grant ANR—16-CE01-0011-01) (J.S.), NSF AGS award 1343077 and 1702266 (B.A.), and NASA award 80NSSC19K1273 (L.J.). The BNP-Paribas foundation is also acknowledged for its financial support under its climate initiative (J.S.). AppSILAS, a scientific program of LEFE-CHAT from the Institut National des Sciences de l'Univers/CNRS, has also provided partial funding for this study (J.S.). S.H. acknowledges JSPS and CNRS under the JSPS–CNRS Joint Research Program. J.S. acknowledges the CNRS/INSU (PRC program 207394) and the PH-SAKURA program of the French Embassy in Japan (project 31897PM) for financial support. Meteo France is acknowledged for providing meteorological data at DDU and IPEV/PNRA for providing routine meteorological observation at station Concordia (www.climantartide.it).

References

Alexander, B., Savarino, J., Barkov, N. I., Delmas, R. J., & Thiemens, M. H. (2002). Climate driven changes in the oxidation pathways of atmospheric sulfur. *Geophysical Research Letters*, *29*(14). https://doi.org/10.1029/2002GL014879

Alexander, B., Thiemens, M. H., Farquhar, J., Kaufman, A. J., Savarino, J., & Delmas, R. J. (2003). East Antarctic ice core sulfur isotope measurements over a complete glacial-interglacial cycle. *Journal of Geophysical Research D: Atmospheres*, *108*(24), 4876. https://doi.org/10.1029/2003jd003513

Alexander, B., Park, R. J., Jacob, D. J., Li, Q. B., Yantosca, R. M., Savarino, J., et al. (2005). Sulfate formation in sea-salt aerosols: Constraints from oxygen isotopes. *Journal of Geophysical Research D: Atmospheres*, *110*(10), 1–12. https://doi.org/10.1029/2004JD005659

Alexander, B., Allman, D. J., Amos, H. M., Fairlie, T. D., Dachs, J., Hegg, D. A., & Sletten, R. S. (2012). Isotopic constraints on the formation pathways of sulfate aerosol in the marine boundary layer of the subtropical northeast Atlantic Ocean. *Journal of Geophysical Research Atmospheres*, *117*(6). https://doi.org/10.1029/2011JD016773

Alexander, B., & Mickley, L. J. (2015). Paleo-Perspectives on Potential Future Changes in the Oxidative Capacity of the Atmosphere Due to Climate Change and Anthropogenic Emissions. *Current Pollution Reports*. Springer. https://doi.org/10.1007/s40726-015-0006-0

Argentini, S., Pietroni, I., Mastrantonio, G., Viola, A. P., Dargaud, G., & Petenko, I. (2014). Observations of near surface wind speed, temperature and radiative budget at Dome C, Antarctic Plateau during 2005. *Antarctic Science*, 26(1), 104–112. https://doi.org/10.1017/S0954102013000382

Bardouki, H., Da Rosa, M. B., Mihalopoulos, N., Palm, W. U., & Zetzsch, C. (2002). Kinetics and mechanism of the oxidation of dimethylsulfoxide (DMSO) and methanesulfinate (MSI-) by OH radicals in aqueous medium. *Atmospheric Environment*, *36*(29), 4627–4634. https://doi.org/10.1016/S1352-2310(02)00460-0

Barkan, E., & Luz, B. (2005). High precision measurements of $^{17}O/^{16}O$ and $^{18}O/^{16}O$ ratios in H_2O. *Rapid Communications in Mass Spectrometry*, *19*(24), 3737–3742. https://doi.org/10.1002/rcm.2250

Barnes, I., Hjorth, J., & Mihalopoulos, N. (2006). Dimethyl Sulfide and Dimethyl Sulfoxide and Their Oxidation in the Atmosphere. https://doi.org/10.1021/CR020529+

Bhattacharya, S. K., Pandey, A., & Savarino, J. (2008). Determination of intramolecular isotope distribution of ozone by oxidation reaction with silver metal. *Journal of Geophysical Research*, *113*(D3). https://doi.org/10.1029/2006jd008309

Bräuer, P., Tilgner, A., Wolke, R., & Herrmann, H. (2013). Mechanism development and modelling of tropospheric multiphase halogen chemistry: The CAPRAM Halogen Module 2.0 (HM2). *Journal of Atmospheric Chemistry*, *70*(1), 19–52. https://doi.org/10.1007/s10874-013-9249-6

Chen, Q., Geng, L., Schmidt, J., Xie, Z., Kang, H., Dachs, J., et al. (2016). Isotopic constraints on the role of hypohalous acids in sulfate aerosol formation in the remote marine boundary layer.

Atmospheric Chemistry and Physics, 16(17), 11433–11450. https://doi.org/10.5194/acp-16-11433-2016

Chen, Q., Schmidt, J. A., Shah, V., Jaeglé, L., Sherwen, T., & Alexander, B. (2017). Sulfate production by reactive bromine: Implications for the global sulfur and reactive bromine budgets. *Geophysical Research Letters*, *44*(13), 7069–7078. https://doi.org/10.1002/2017GL073812

Chen, Q., Sherwen, T., Evans, M., & Alexander, B. (2018). DMS oxidation and sulfur aerosol formation in the marine troposphere: a focus on reactive halogen and multiphase chemistry. *Atmospheric Chemistry and Physics*, *18*(18), 13617–13637. https://doi.org/10.5194/acp-18-13617-2018

Cosme, E., Hourdin, F., Genthon, C., & Martinerie, P. (2005). Origin of dimethylsulfide, non-sea-salt sulfate, and methanesulfonic acid in eastern Antarctica. *Journal of Geophysical Research D: Atmospheres*, *110*(3), 1–17. https://doi.org/10.1029/2004JD004881

Crawford, J. H., Davis, D. D., Chen, G., Buhr, M., Oltmans, S., Weller, R., et al. (2001). Evidence for photochemical production of ozone at the South Pole surface. *Geophysical Research Letters*, *28*(19), 3641–3644. https://doi.org/10.1029/2001GL013055

Delmas, R. J., Wagnon, P., Goto-Azuma, K., Kamiyama, K., & Watanabe, O. (2003). Evidence for the loss of snow-deposited MSA to the interstitial gaseous phase in central Antarctic firn. *Tellus B: Chemical and Physical Meteorology*, *55*(1), 71–79. https://doi.org/10.3402/tellusb.v55i1.16355

Dubey, M. K., Mohrschladt, R., Donahue, N. M., & Anderson, J. G. (1997). Isotope specific kinetics of hydroxyl radical (OH) with water (H_2O): Testing models of reactivity and atmospheric fractionation. *Journal of Physical Chemistry A*, *101*(8), 1494–1500. https://doi.org/10.1021/jp962332p

Elsässer, C., Wagenbach, D., Weller, R., Auer, M., Wallner, A., & Christl, M. (2011). Continuous 25-yr aerosol records at coastal Antarctica: Part 2: Variability of the radionuclides 7Be, 10Be 210Pb. *Tellus, Series B: Chemical and Physical Meteorology*, *63*(5), 920–934. https://doi.org/10.1111/j.1600-0889.2011.00543.x

Erbland, J., Vicars, W. C., Savarino, J., Morin, S., Frey, M. M., Frosini, D., et al. (2013). Air-snow transfer of nitrate on the East Antarctic Plateau - Part 1: Isotopic evidence for a photolytically driven dynamic equilibrium in summer. *Atmospheric Chemistry and Physics*, *13*(13), 6403–6419. https://doi.org/10.5194/acp-13-6403-2013

Ervens, B., George, C., Williams, J. E., Buxton, G. V., Salmon, G. A., Bydder, M., et al. (2003). CAPRAM 2.4 (MODAC mechanism): An extended and condensed tropospheric aqueous phase mechanism and its application. *Journal of Geophysical Research D: Atmospheres*, *108*(14). https://doi.org/10.1029/2002jd002202

Flyunt, R., Makogon, O., Schuchmann, M. N., Asmus, K. D., & Von Sonntag, C. (2001). OH-radical-induced oxidation of methanesulfinic acid. The reactions of the methanesulfonyl radical in the absence and presence of dioxygen. *Journal of the Chemical Society, Perkin Transactions 2*, (5), 787–792. https://doi.org/10.1039/b009631h

Fogelman, K. D., Walker, D. M., & Margerum, D. W. (1989). Non-Metal Redox Kinetics: Hypochlorite and Hypochlorous Acid Reactions with Sulfite. *Inorganic Chemistry*, *28*(6), 986–993. https://doi.org/10.1021/ic00305a002

Frey, M. M., Savarino, J., Morin, S., Erbland, J., & Martins, J. M. F. (2009). Photolysis imprint in the nitrate stable isotope signal in snow and atmosphere of East Antarctica and implications for reactive nitrogen cycling. *Atmospheric Chemistry and Physics*, *9*(22), 8681–8696. https://doi.org/10.5194/acp-9-8681-2009

Geng, L., Schauer, A. J., Kunasek, S. A., Sofen, E. D., Erbland, J., Savarino, J., et al. (2013). Analysis of oxygen-17 excess of nitrate and sulfate at sub-micromole levels using the pyrolysis method. *Rapid Communications in Mass Spectrometry*, *27*(21), 2411–2419. https://doi.org/10.1002/rcm.6703

Gershenzon, M., Davidovits, P., Jayne, J. T., Kolb, C. E., & Worsnop, D. R. (2001). Simultaneous uptake of DMS and ozone on water. *Journal of Physical Chemistry A*, *105*(29), 7031–7036. https://doi.org/10.1021/jp010696y

González-García, N., González-Lafont, A., & Lluch, J. M. (2007). Methanesulfinic acid reaction with OH: Mechanism, rate constants, and atmospheric implications. *Journal of Physical Chemistry A*, *111*(32), 7825–7832. https://doi.org/10.1021/jp0722455

Goto-Azuma, K., Hirabayashi, M., Motoyama, H., Miyake, T., Kuramoto, T., Uemura, R., et al. (2019). Reduced marine phytoplankton sulphur emissions in the Southern Ocean during the past seven glacials. *Nature Communications*, *10*(1). https://doi.org/10.1038/s41467-019-11128-6

Grannas, A. M., Jones, A. E., Dibb, J., Ammann, M., Anastasio, C., Beine, H. J., et al. (2007). An overview of snow photochemistry: evidence, mechanisms and impacts. *Atmospheric Chemistry and Physics*, *7*(16), 4329–4373. https://doi.org/10.5194/acp-7-4329-2007

Grilli, R., Legrand, M., Kukui, A., Méjean, G., Preunkert, S., & Romanini, D. (2013). First investigations of IO, BrO, and NO_2 summer atmospheric levels at a coastal East Antarctic site using mode-locked cavity enhanced absorption spectroscopy. Geophysical Research Letters, 40(4), 791–796. https://doi.org/10.1002/grl.50154

Hill-Falkenthal, J., Priyadarshi, A., Savarino, J., & Thiemens, M. (2013). Seasonal variations in ^{35}S and $\Delta^{17}O$ of sulfate aerosols on the Antarctic plateau. *Journal of Geophysical Research Atmospheres*, *118*(16), 9444–9455. https://doi.org/10.1002/jgrd.50716

Hoffmann, E. H., Tilgner, A., Schrödner, R., Bräuer, P., Wolke, R., & Herrmann, H. (2016). An advanced modeling study on the impacts and atmospheric implications of multiphase dimethyl sulfide chemistry. *Proceedings of the National Academy of Sciences of the United States of America*, *113*(42), 11776–11781. https://doi.org/10.1073/pnas.1606320113

Holland, H. D., Lazar, B., & McCaffrey, M. (1986). Evolution of the atmosphere and oceans. *Nature*, *320*(6057), 27–33. https://doi.org/10.1038/320027a0

Holt, B. D., Kumar, R., & Cunningham, P. T. (1981). Oxygen-18 study of the aqueous-phase oxidation of sulfur dioxide. *Atmospheric Environment (1967)*, *15*(4), 557–566. https://doi.org/10.1016/0004-6981(81)90186-4

Huang, J., & Jaeglé, L. (2017). Wintertime enhancements of sea salt aerosol in polar regions consistent with a sea ice source from blowing snow. *Atmospheric Chemistry and Physics*, 17(5), 3699–3712. https://doi.org/10.5194/acp-17-3699-2017

Huang, J., Jaeglé, L., & Shah, V. (2018). Using CALIOP to constrain blowing snow emissions of sea salt aerosols over Arctic and Antarctic sea ice. *Atmospheric Chemistry and Physics*, *18*(22), 16253–16269. https://doi.org/10.5194/acp-18-16253-2018

Huang, J., Jaeglé, L., Chen, Q., Alexander, B., Sherwen, T., Evans, M. J., et al. (2020). Evaluating the impact of blowing-snow sea salt aerosol on springtime BrO and O_3 in the Arctic. *Atmospheric Chemistry and Physics*, 20(12), 7335–7358. https://doi.org/10.5194/acp-20-7335-2020

Ingham, T., Bauer, D., Sander, R., Crutzen, P. J., & Crowley, J. N. (1999). Kinetics and Products of the Reactions BrO + DMS and Br + DMS at 298 K. *Journal of Physical Chemistry A*, *103*(36), 7199–7209. https://doi.org/10.1021/jp9905979

Ishino, S., Hattori, S., Savarino, J., Jourdain, B., Preunkert, S., Legrand, M., et al. (2017). Seasonal variations of triple oxygen isotopic compositions of atmospheric sulfate, nitrate, and ozone at Dumont d'Urville, coastal Antarctica. *Atmospheric Chemistry and Physics*, *17*(5), 3713–3727. https://doi.org/10.5194/acp-17-3713-2017

Ishino, S., Hattori, S., Savarino, J., Legrand, M., Albalat, E., Albarede, F., et al. (2019). Homogeneous sulfur isotope signature in East Antarctica and implication for sulfur source shifts through the last glacial-interglacial cycle. *Scientific Reports*, *9*(1), 12378. https://doi.org/10.1038/s41598-019-48801-1

Jaeglé, L., Quinn, P. K., Bates, T. S., Alexander, B., & Lin, J.-T. (2011). Global distribution of sea salt aerosols: new constraints from in situ and remote sensing observations. *Atmos. Chem. Phys.*, *11*(7), 3137–3157. https://doi.org/10.5194/acp-11-3137-2011

Janssen, C., Guenther, J., Krankowsky, D., & Mauersberger, K. (2003). Temperature dependence of ozone rate coefficients and isotopologue fractionation in ^{16}O-^{18}O oxygen mixtures. *Chemical Physics Letters*, *367*(1–2), 34–38. https://doi.org/10.1016/S0009-2614(02)01665-2

Janssen, C., & Tuzson, B. (2006). A diode laser spectrometer for symmetry selective detection of ozone isotopomers. *Applied Physics B: Lasers and Optics*, *82*(3), 487–494. https://doi.org/10.1007/s00340-005-2044-6

Jeffery, C. A., & Austin, P. H. (1997). Homogeneous nucleation of supercooled water: Results from a new equation of state. *Journal of Geophysical Research Atmospheres*, *102*(21), 25269–25279. https://doi.org/10.1029/97jd02243

Johnston, J. C., & Thiemens, M. H. (1997). The isotopic composition of tropospheric ozone in three environments. *Journal of Geophysical Research Atmospheres*, *102*(21), 25395–25404. https://doi.org/10.1029/97jd02075

Jourdain, B., & Legrand, M. (2002). Year-round records of bulk and size-segregated aerosol composition and HCl and HNO_3 levels in the Dumont d'Urville (coastal Antarctica) atmosphere: Implications for sea-salt aerosol fractionation in the winter and summer. *Journal of Geophysical Research Atmospheres*, *107*(22). https://doi.org/10.1029/2002JD002471

Krankowsky, D., Bartecki, F., Klees, G. G., Mauersberger, K., Schellenbach, K., & Stehr, J. (1995). Measurement of heavy isotope enrichment in tropospheric ozone. *Geophysical Research Letters*, *22*(13), 1713–1716. https://doi.org/10.1029/95GL01436

Kukui, A., Bossoutrot, V., Laverdet, G., & Le Bras, G. (2000). Mechanism of the reaction of CH_3SO with NO_2 in relation to atmospheric oxidation of dimethyl sulfide: Experimental and theoretical study. *Journal of Physical Chemistry A*, *104*(5), 935–946. https://doi.org/10.1021/jp993158i

Kunasek, S. A., Alexander, B., Steig, E. J., Sofen, E. D., Jackson, T. L., Thiemens, M. H., et al. (2010). Sulfate sources and oxidation chemistry over the past 230 years from sulfur and oxygen isotopes of sulfate in a West Antarctic ice core. *Journal of Geophysical Research Atmospheres*, *115*(18). https://doi.org/10.1029/2010JD013846

Lana, A., Bell, T. G., Simó, R., Vallina, S. M., Ballabrera-Poy, J., Kettle, A. J., et al. (2011). An updated climatology of surface dimethlysulfide concentrations and emission fluxes in the global ocean. *Global Biogeochemical Cycles*, 25(1), n/a-n/a. https://doi.org/10.1029/2010GB003850

Legrand, M. R., Delmas, R. J., & Charlson, R. J. (1988). Climate forcing implications from Vostok ice-core sulphate data. *Nature*, *334*(6181), 418–420. https://doi.org/10.1038/334418a0

Legrand, M., & Mayewski, P. (1997). Glaciochemistry of polar ice cores: A review. *Reviews of Geophysics*, 35(3), 219–243. Blackwell Publishing Ltd. https://doi.org/10.1029/96RG03527

Legrand, M., Preunkert, S., Savarino, J., Frey, M. M., Kukui, A., Helmig, D., et al. (2016a). Inter-annual variability of surface ozone at coastal (Dumont d'Urville, 2004-2014) and inland (Concordia, 2007-2014) sites in East Antarctica. *Atmospheric Chemistry and Physics*, *16*(12), 8053–8069. https://doi.org/10.5194/acp-16-8053-2016

Legrand, M., Yang, X., Preunkert, S., & Theys, N. (2016b). Year-round records of sea salt, gaseous, and particulate inorganic bromine in the atmospheric boundary layer at coastal (Dumont d'Urville) and central (Concordia) East Antarctic sites. *Journal of Geophysical Research: Atmospheres*, *121*(2), 997–1023. https://doi.org/10.1002/2015JD024066

Legrand, M., Preunkert, S., Wolff, E., Weller, R., Jourdain, B., & Wagenbach, D. (2017a). Year-round records of bulk and size-segregated aerosol composition in central Antarctica (Concordia site) - Part 1: Fractionation of sea-salt particles. *Atmospheric Chemistry and Physics*, *17*(22), 14039–14054. https://doi.org/10.5194/acp-17-14039-2017

Legrand, M., Preunkert, S., Weller, R., Zipf, L., Elsässer, C., Merchel, S., et al. (2017b). Year-round record of bulk and size-segregated aerosol composition in central Antarctica (Concordia site) – Part 2: Biogenic sulfur (sulfate and methanesulfonate) aerosol. *Atmospheric Chemistry and Physics*, *17*(22), 14055–14073. https://doi.org/10.5194/acp-17-14055-2017

Listowski, C., Delanoë, J., Kirchgaessner, A., Lachlan-Cope, T., & King, J. (2019). Antarctic clouds, supercooled liquid water and mixed phase, investigated with DARDAR: geographical and seasonal variations. *Atmospheric Chemistry and Physics*, *19*(10), 6771–6808. https://doi.org/10.5194/acp-19-6771-2019

Liu, T., & Abbatt, J. P. D. (2020). An Experimental Assessment of the Importance of S(IV) Oxidation by Hypohalous Acids in the Marine Atmosphere. *Geophysical Research Letters*, *47*(4). https://doi.org/10.1029/2019GL086465

Liu, Q., Schurter, L. M., Muller, C. E., Aloisio, S., Francisco, J. S., & Margerum, D. W. (2001). Kinetics and mechanisms of aqueous ozone reactions with bromide, sulfite, hydrogen sulfite, iodide, and nitrite ions. *Inorganic Chemistry*, *40*(17), 4436–4442. https://doi.org/10.1021/ic000919j

997 Lyons, J. R. (2001). Transfer of mass-independent fractionation in ozone to other oxygen-
998 containing radicals in the atmosphere. *Geophysical Research Letters*, *28*(17), 3231–3234.
999 https://doi.org/10.1029/2000GL012791

1000 Matsuhisa, Y., Goldsmith, J. R., & Clayton, R. N. (1979). Oxygen isotopic fractionation in the
1001 system quartz-albite-anorthite-water. *Geochimica et Cosmochimica Acta*, *43*(7), 1131–1140.
1002 https://doi.org/https://doi.org/10.1016/0016-7037(79)90099-1

1003 Mauersberger, K., Krankowsky, D., & Janssen, C. (2003). *Oxygen Isotope Processes and*
1004 *Transfer Reactions* (pp. 265–279). Springer, Dordrecht. https://doi.org/10.1007/978-94-010-
1005 0145-8_17

1006 Mauldin, R. L., Eisele, F. L., Tanner, D. J., Kosciuch, E., Shetter, R., Lefer, B., et al. (2001).
1007 Measurements of OH, H_2SO_4 and MSA at the South Pole during ISCAT. *Geophysical Research*
1008 *Letters*, *28*(19), 3629–3632. https://doi.org/10.1029/2000GL012711

1009 Minikin, A., Legrand, M., Hall, J., Wagenbach, D., Kleefeld, C., Wolff, E., et al. (1998). Sulfur-
1010 containing species (sulfate and methanesulfonate) in coastal Antarctic aerosol and precipitation.
1011 *Journal of Geophysical Research D: Atmospheres*, *103*(3339), 10975–10990.
1012 https://doi.org/10.1029/98jd00249

1013 Morin, S., Savarino, J., Bekki, S., Gong, S., & Bottenheim, J. W. (2007). Signature of Arctic
1014 surface ozone depletion events in the isotope anomaly ($\Delta^{17}O$) of atmospheric nitrate.
1015 *Atmospheric Chemistry and Physics*, *7*(5), 1451–1469. https://doi.org/10.5194/acp-7-1451-2007

1016 Morton, J., Barnes, J., Schueler, B., & Mauersberger, K. (1990). Laboratory studies of heavy
1017 ozone. *Journal of Geophysical Research*, *95*(D1), 901–907.
1018 https://doi.org/10.1029/JD095iD01p00901

1019 Mungall, E. L., Wong, J. P. S., & Abbatt, J. P. D. (2018). Heterogeneous Oxidation of Particulate
1020 Methanesulfonic Acid by the Hydroxyl Radical: Kinetics and Atmospheric Implications. *ACS*
1021 *Earth and Space Chemistry*, 2(1), 48–55. https://doi.org/10.1021/acsearthspacechem.7b00114

1022 Murray, L. T., Mickley, L. J., Kaplan, J. O., Sofen, E. D., Pfeiffer, M., & Alexander, B. (2014).
1023 Factors controlling variability in the oxidative capacity of the troposphere since the Last Glacial
1024 Maximum. *Atmospheric Chemistry and Physics*, *14*(7), 3589–3622. https://doi.org/10.5194/acp-
1025 14-3589-2014

1026 Noro, K., Hattori, S., Uemura, R., Fukui, K., Hirabayashi, M., Kawamura, K., Motoyama, H.,
1027 Takenaka, N., & Yoshida, N. (2018). Spatial variation of isotopic compositions of snowpack
1028 nitrate related to post-depositional processes in eastern Dronning Maud Land, East Antarctica.
1029 *GEOCHEMICAL JOURNAL*, *52*(2), e7–e14. https://doi.org/10.2343/geochemj.2.0519

1030 Park, R. J., Jacob, D. J., Field, B. D., & Yantosca, R. M. (2004). Natural and transboundary
1031 pollution influences on sulfate-nitrate-ammonium aerosols in the United States: Implications for
1032 policy. *Journal of Geophysical Research*, *109*(D15). https://doi.org/10.1029/2003jd004473

1033 Parrella, J. P., Jacob, D. J., Liang, Q., Zhang, Y., Mickley, L. J., Miller, B., et al. (2012).
1034 Tropospheric bromine chemistry: Implications for present and pre-industrial ozone and mercury.
1035 *Atmospheric Chemistry and Physics*, *12*(15), 6723–6740. https://doi.org/10.5194/acp-12-6723-
1036 2012

Patris, N., Delmas, R. J., & Jouzel, J. (2000). Isotopic signatures of sulfur in shallow Antarctic ice cores. *Journal of Geophysical Research Atmospheres*, *105*(D6), 7071–7078. https://doi.org/10.1029/1999JD900974

Pound, R. J., Sherwen, T., Helmig, D., Carpenter, L. J., & Evans, M. J. (2020). Influences of oceanic ozone deposition on tropospheric photochemistry. *Atmospheric Chemistry and Physics*, *20*(7), 4227–4239. https://doi.org/10.5194/acp-20-4227-2020

Preunkert, S., Legrand, M., Jourdin, B., Moulin, C., Belviso, S., Kasamatsu, N., et al. (2007). Interannual variability of dimethylsulfide in air and seawater and its atmospheric oxidation by-products (methanesulfonate and sulfate) at Dumont d'Urville, coastal Antarctica (1999-2003). *Journal of Geophysical Research Atmospheres*, *112*(6). https://doi.org/10.1029/2006JD007585

Preunkert, S., Jourdain, B., Legrand, M., Udisti, R., Becagli, S., & Cerri, O. (2008). Seasonality of sulfur species (dimethyl sulfide, sulfate, and methanesulfonate) in Antarctica: Inland versus coastal regions. *Journal of Geophysical Research Atmospheres*, *113*(15). https://doi.org/10.1029/2008JD009937

Pruett, L. E., Kreutz, K. J., Wadleigh, M., & Aizen, V. (2004). Assessment of sulfate sources in high-elevation Asian precipitation using stable sulfur isotopes. *Environmental Science and Technology*, *38*(18), 4728–4733. https://doi.org/10.1021/es035156o

Pruppacher, H. R. (1995). A New Look at Homogeneous Ice Nucleation in Supercooled Water Drops. *Journal of the Atmospheric Sciences*, *52*(11), 1924–1933. https://doi.org/10.1175/1520-0469(1995)052<1924:ANLAHI>2.0.CO;2

Riley, J. P. & Chester, R. (1971). Introduction to Marine Chemistry, Academic Press, London and New York.

Saiz-Lopez, A., Mahajan, A. S., Salmon, R. A., Bauguitte, S. J. B., Jones, A. E., Roscoe, H. K., & Plane, J. M. C. (2007). Boundary layer halogens in coastal Antarctica. *Science*, *317*(5836), 348–351. https://doi.org/10.1126/science.1141408

Savarino, J., & Thiemens, M. H. (1999). Analytical procedure to determine both $\delta^{18}O$ and $\delta^{17}O$ of H_2O_2 in natural water and first measurements. *Atmospheric Environment*, *33*(22), 3683–3690. https://doi.org/10.1016/S1352-2310(99)00122-3

Savarino, J., Lee, C. C. W., & Thiemens, M. H. (2000). Laboratory oxygen isotopic study of sulfur (IV) oxidation: Origin of the mass-independent oxygen isotopic anomaly in atmospheric sulfates and sulfate mineral deposits on Earth. *Journal of Geophysical Research: Atmospheres*, *105*(D23), 29079–29088. https://doi.org/10.1029/2000JD900456

Savarino, J., Alexander, B., Darmohusodo, V., & Thiemens, M. H. (2001). Sulfur and oxygen isotope analysis of sulfate at micromole levels using a pyrolysis technique in a continuous flow system. *Analytical Chemistry*, *73*(18), 4457–4462. https://doi.org/10.1021/ac010017f

Savarino, J., Vicars, W. C., Legrand, M., Preunkert, S., Jourdain, B., Frey, M. M., Kukui, A., Caillon, N., & Gil Roca, J. (2016). Oxygen isotope mass balance of atmospheric nitrate at Dome C, East Antarctica, during the OPALE campaign. *Atmospheric Chemistry and Physics*, *16*(4), 2659–2673. https://doi.org/10.5194/acp-16-2659-2016

Schauer, A. J., Kunasek, S. A., Sofen, E. D., Erbland, J., Savarino, J., Johnson, B. W., et al. (2012). Oxygen isotope exchange with quartz during pyrolysis of silver sulfate and silver nitrate.

Rapid Communications in Mass Spectrometry, *26*(18), 2151–2157. https://doi.org/10.1002/rcm.6332

Schmidt, J. A., Jacob, D. J., Horowitz, H. M., Hu, L., Sherwen, T., Evans, M. J., et al. (2016). Modeling the observed tropospheric BrO background: Importance of multiphase chemistry and implications for ozone, OH, andmercury. *Journal of Geophysical Research*, *121*(19), 11819–11835. https://doi.org/10.1002/2015JD024229

Seinfeld, J. H., & Pandis, S. N. (2006). Atmospheric chemistry and physics: from air pollution to climate change. *Atmospheric Chemistry and Physics: From Air Pollution to Climate Change.*

Shaheen, R., Abauanza, M., Jackson, T. L., McCabe, J., Savarino, J., & Thiemens, M. H. (2013). Tales of volcanoes and El-Niño southern oscillations with the oxygen isotope anomaly of sulfate aerosol. *Proceedings of the National Academy of Sciences of the United States of America*, *110*(44), 17662–17667. https://doi.org/10.1073/pnas.1213149110

Sherwen, T., Evans, M. J., Carpenter, L. J., Andrews, S. J., Lidster, R. T., Dix, B., et al. (2016a). Iodine's impact on tropospheric oxidants: a global model study in GEOS-Chem. *Atmospheric Chemistry and Physics*, *16*(2), 1161–1186. https://doi.org/10.5194/acp-16-1161-2016

Sherwen, T., Schmidt, J. A., Evans, M. J., Carpenter, L. J., Großmann, K., Eastham, S. D., et al. (2016b). Global impacts of tropospheric halogens (Cl, Br, I) on oxidants and composition in GEOS-Chem. *Atmospheric Chemistry and Physics*, *16*(18), 12239–12271. https://doi.org/10.5194/acp-16-12239-2016

Simpson, W. R., Von Glasow, R., Riedel, K., Anderson, P., Ariya, P., Bottenheim, J., et al. (2007). Halogens and their role in polar boundary-layer ozone depletion. *Atmospheric Chemistry and Physics*, *7*(16), 4375–4418. https://doi.org/10.5194/acp-7-4375-2007

Sofen, E. D., Alexander, B., Steig, E. J., Thiemens, M. H., Kunasek, S. A., Amos, H. M., et al. (2014). WAIS Divide ice core suggests sustained changes in the atmospheric formation pathways of sulfate and nitrate since the 19th century in the extratropical Southern Hemisphere. *Atmospheric Chemistry and Physics*, *14*(11), 5749–5769. https://doi.org/10.5194/acp-14-5749-2014

Tian, Y., Tian, Z. M., Wei, W. M., He, T. J., Chen, D. M., & Liu, F. C. (2007). Ab initio study of the reaction of OH radical with methyl sulfinic acid (MSIA). *Chemical Physics*, *335*(2–3), 133–140. https://doi.org/10.1016/j.chemphys.2007.04.009

Theys, N., Van Roozendael, M., Hendrick, F., Yang, X., De Smedt, I., Richter, A., et al. (2011). Global observations of tropospheric BrO columns using GOME-2 satellite data. *Atmospheric Chemistry and Physics*, 11(4), 1791–1811. https://doi.org/10.5194/acp-11-1791-2011

Thiemens, M. H., & Jackson, T. (1990). Pressure dependency for heavy isotope enhancement in ozone formation. *Geophysical Research Letters*, *17*(6), 717–719. https://doi.org/10.1029/GL017i006p00717

Troy, R. C., & Margerum, D. W. (1991). Non-Metal Redox Kinetics: Hypobromite and Hypobromous Acid Reactions with Iodide and with Sulfite and the Hydrolysis of Bromosulfate. *Inorganic Chemistry*, *30*(18), 3538–3543. https://doi.org/10.1021/ic00018a028

Vicars, W. C., & Savarino, J. (2014). Quantitative constraints on the ^{17}O-excess (Δ^{17}O) signature of surface ozone: Ambient measurements from 50°N to 50°S using the nitrite-coated filter

technique. *Geochimica et Cosmochimica Acta*, *135*, 270–287. https://doi.org/10.1016/j.gca.2014.03.023

von Glasow, R., & Crutzen, P. J. (2004). Model study of multiphase DMS oxidation with a focus on halogens. *Atmospheric Chemistry and Physics*, *4*(3), 589–608. https://doi.org/10.5194/acp-4-589-2004

Wagenbach, D., Ducroz, F., Mulvaney, R., Keck, L., Minikin, A., Legrand, M., et al. (1998). Sea-salt aerosol in coastal Antarctic regions. *Journal of Geophysical Research D: Atmospheres*, *103*(3339), 10961–10974. https://doi.org/10.1029/97jd01804

Wagnon, P., Delmas, R. J., & Legrand, M. (1999). Loss of volatile acid species from upper firn layers at Vostok, Antarctica. *Journal of Geophysical Research: Atmospheres*, *104*(D3), 3423–3431. https://doi.org/10.1029/98JD02855

Walters, W. W., Michalski, G., Böhlke, J. K., Alexander, B., Savarino, J., & Thiemens, M. H. (2019). Assessing the Seasonal Dynamics of Nitrate and Sulfate Aerosols at the South Pole Utilizing Stable Isotopes. *Journal of Geophysical Research: Atmospheres*, *124*(14), 8161–8177. https://doi.org/10.1029/2019JD030517

Wang, L., & Zhang, J. (2002). Ab initio study of reaction of dimethyl sulfoxide (DMSO) with OH radical. *Chemical Physics Letters*, *356*(5–6), 490–496. https://doi.org/10.1016/S0009-2614(02)00397-4

Weller, R., Traufetter, F., Fischer, H., Oerter, H., Piel, C., & Miller, H. (2004). Postdepositional losses of methane sulfonate, nitrate, and chloride at the European Project for Ice Coring in Antarctica deep-drilling site in Dronning Maud Land, Antarctica. *Journal of Geophysical Research D: Atmospheres*, *109*(7). https://doi.org/10.1029/2003jd004189

Wolff, E. W., Fischer, H., Fundel, F., Ruth, U., Twarloh, B., Littot, G. C., et al. (2006). Southern Ocean sea-ice extent, productivity and iron flux over the past eight glacial cycles. *Nature*, *440*(7083), 491–496. https://doi.org/10.1038/nature04614

Yang, X., Pyle, J. A., & Cox, R. A. (2008). Sea salt aerosol production and bromine release: Role of snow on sea ice. *Geophysical Research Letters*, *35*(16). https://doi.org/10.1029/2008GL034536

Zatko, M., Geng, L., Alexander, B., Sofen, E., & Klein, K. (2016). The impact of snow nitrate photolysis on boundary layer chemistry and the recycling and redistribution of reactive nitrogen across Antarctica and Greenland in a global chemical transport model. *Atmospheric Chemistry and Physics*, *16*(5), 2819–2842. https://doi.org/10.5194/acp-16-2819-2016

Zhang, J., Miau, T.-T., & Lee, Y. T. (1997). Crossed Molecular Beam Study of the Reaction Br + O_3[†]. *The Journal of Physical Chemistry A*, *101*(37), 6922–6930. https://doi.org/10.1021/jp970860a

Zhu, L., Michael Nicovich, J., & Wine, P. H. (2003a). Temperature-dependent kinetics studies of aqueous phase reactions of hydroxyl radicals with dimethylsulfoxide, dimethylsulfone, and methanesulfonate. *Aquatic Sciences*, *65*(4), 425–435. https://doi.org/10.1007/s00027-003-0673-6

Zhu, L., Nicovich, J. M., & Wine, P. H. (2003b). Temperature-dependent kinetics studies of aqueous phase reactions of SO_4^- radicals with dimethylsulfoxide, dimethylsulfone, and

1159 methanesulfonate. *Journal of Photochemistry and Photobiology A: Chemistry*, *157*(2–3), 311–
1160 319. https://doi.org/10.1016/S1010-6030(03)00064-9

1161 Zhu, L. (2004). *AQUEOUS PHASE REACTION KINETICS OF ORGANIC SULFUR*
1162 *COMPOUNDS OF ATMOSPHERIC INTEREST*. A dissertation in Georgia Institute of
1163 Technology. https://smartech.gatech.edu/handle/1853/4870

Figure1.

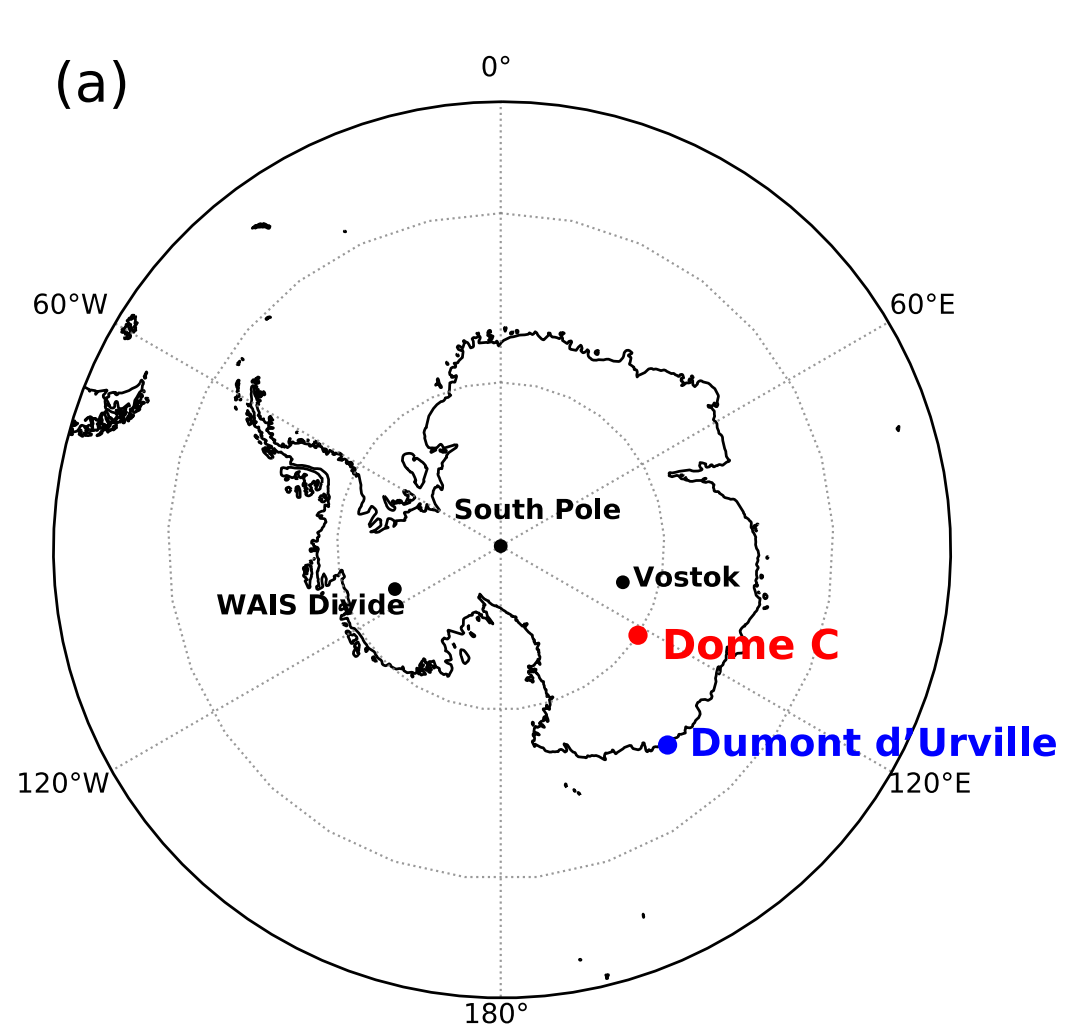
(a)
0°
60°W
60°E
120°W
120°E
180°
South Pole
Vostok
WAIS Divide
Dome C
Dumont d'Urville

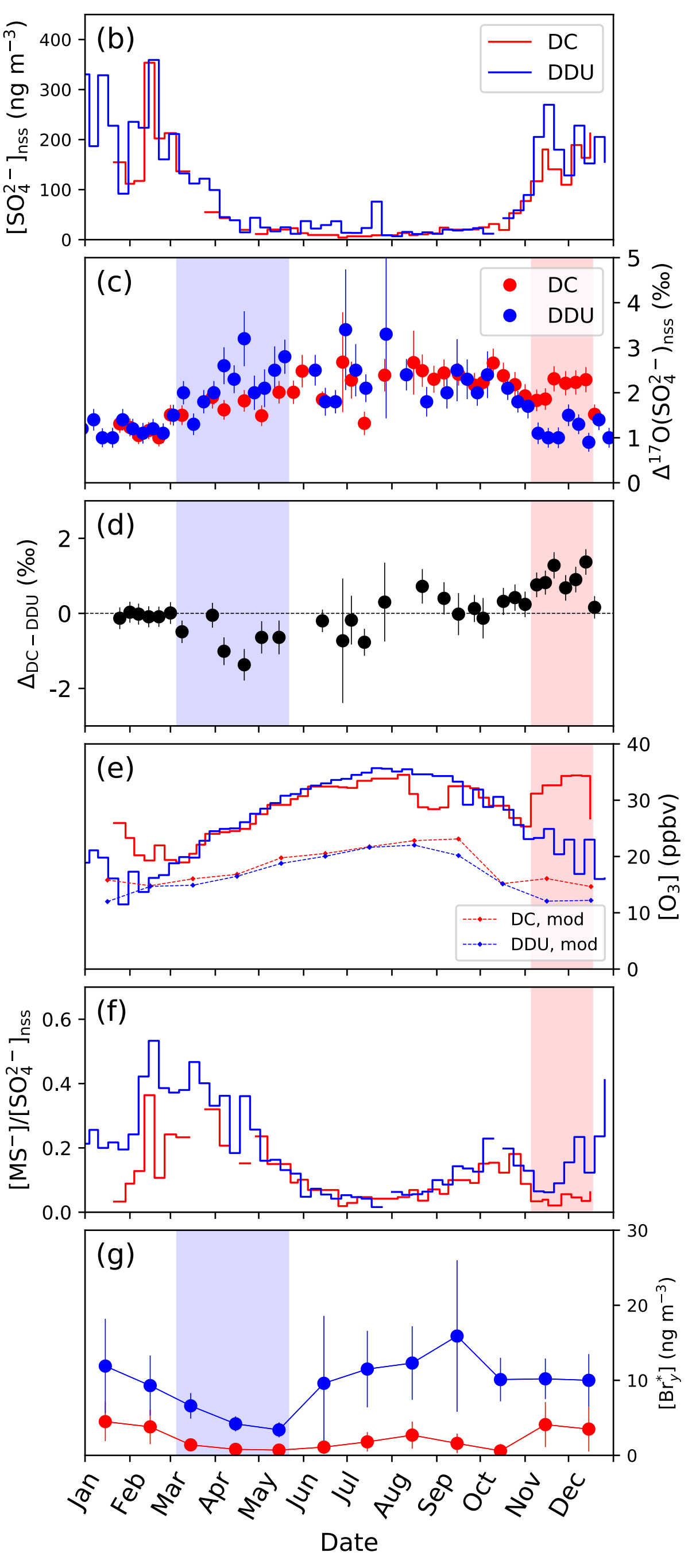
(b)
DC
DDU
$[SO_4^{2-}]_{nss}$ (ng m^{-3})
(c)
$\Delta^{17}O(SO_4^{2-})_{nss}$ (‰)
(d)
Δ_{DC-DDU} (‰)
(e)
DC, mod
DDU, mod
$[O_3]$ (ppbv)
(f)
$[MS^-]/[SO_4^{2-}]_{nss}$
(g)
$[Br_y^*]$ (ng m^{-3})
Jan
Feb
Mar
Apr
May
Jun
Jul
Aug
Sep
Oct
Nov
Dec
Date

Figure2.

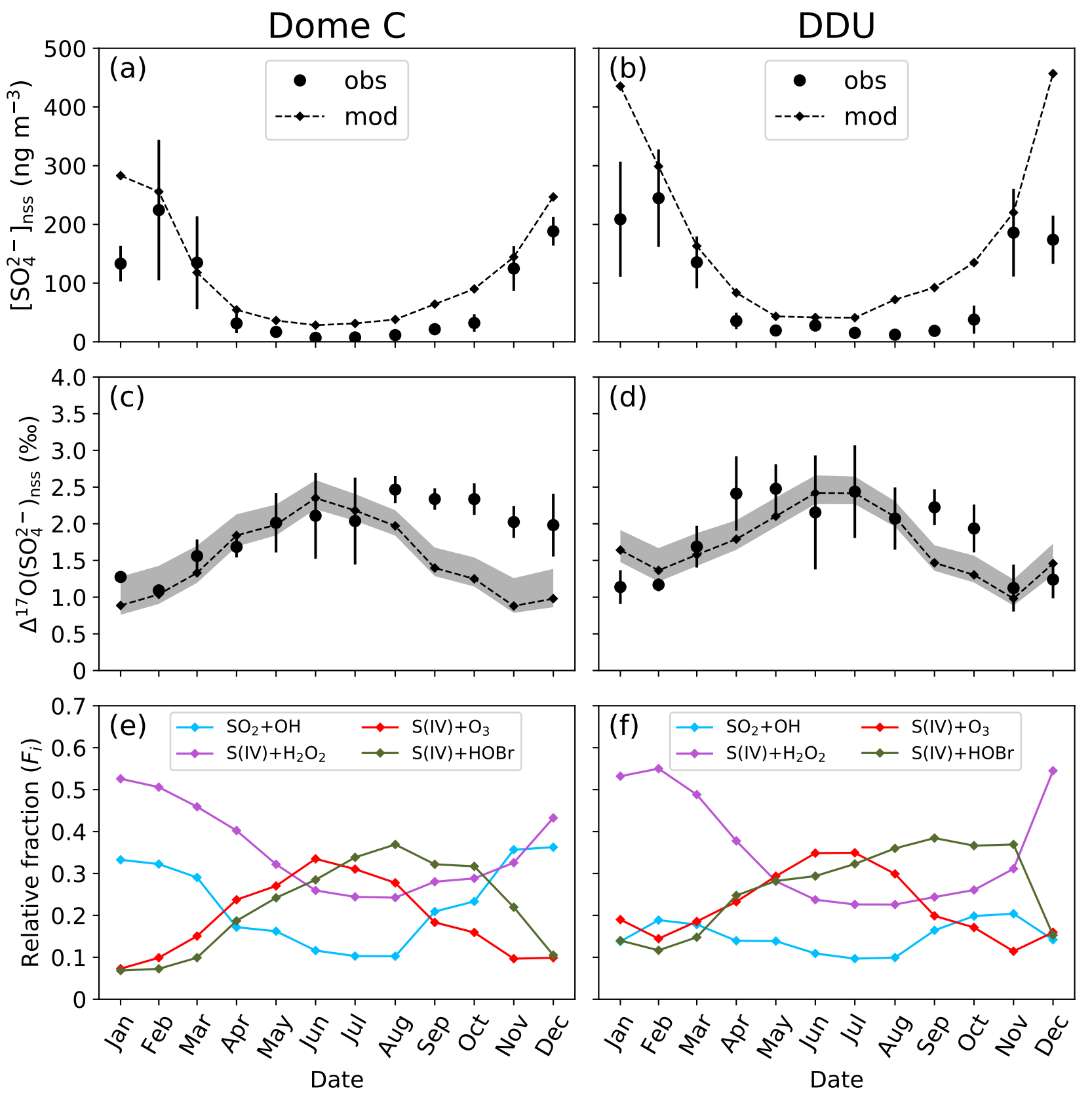
Dome C
DDU
(a)
(b)
(c)
(d)
(e)
(f)
obs
mod
$[SO_4^{2-}]_{nss}$ (ng m^{-3})
$\Delta^{17}O(SO_4^{2-})_{nss}$ (‰)
Relative fraction (F_i)
SO_2+OH
S(IV)+O_3
S(IV)+H_2O_2
S(IV)+HOBr
Jan
Feb
Mar
Apr
May
Jun
Jul
Aug
Sep
Oct
Nov
Dec
Date

Figure3.

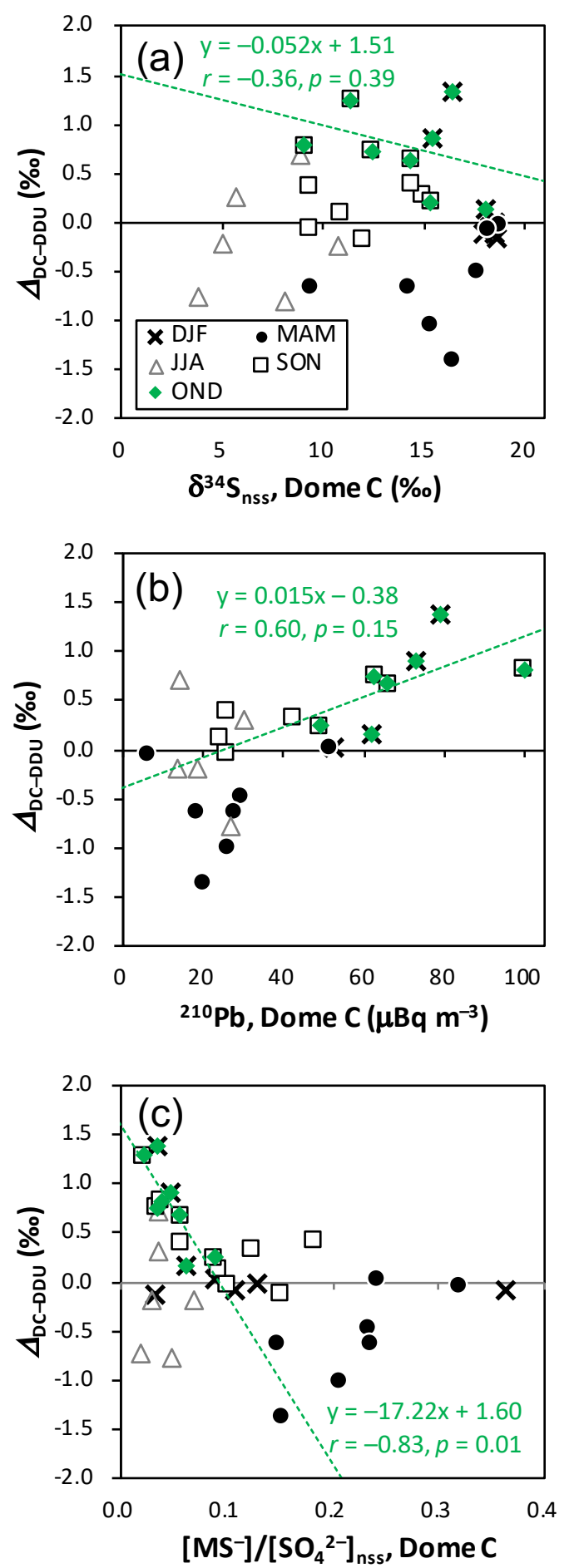
(a)
y = –0.052x + 1.51
r = –0.36, p = 0.39
DJF
MAM
JJA
SON
OND
Δ DC–DDU (‰)
δ34Snss, Dome C (‰)
(b)
y = 0.015x – 0.38
r = 0.60, p = 0.15
Δ DC–DDU (‰)
210Pb, Dome C (μBq m–3)
(c)
y = –17.22x + 1.60
r = –0.83, p = 0.01
Δ DC–DDU (‰)
[MS–]/[SO42–]nss, Dome C

Figure4.

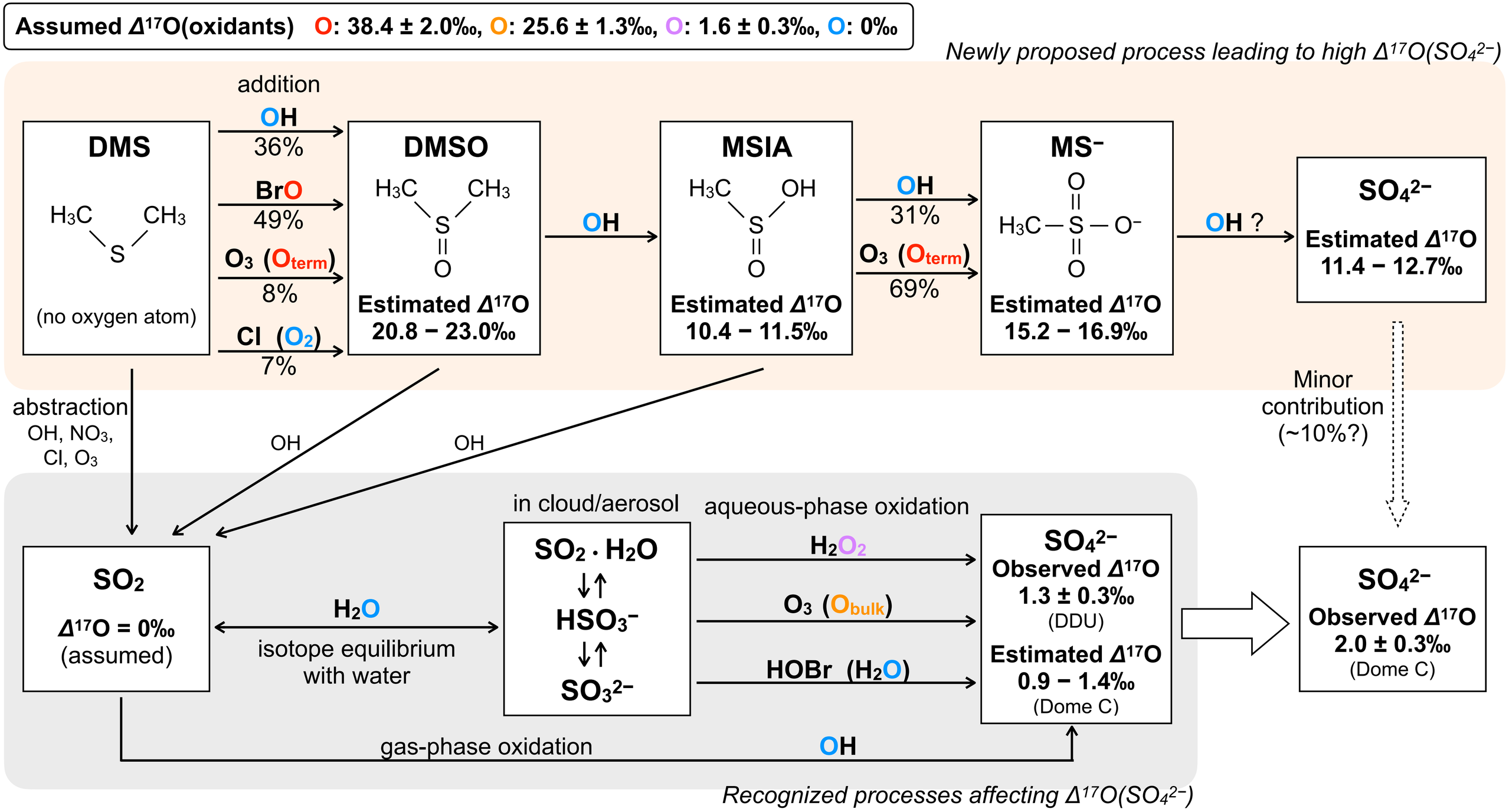
Assumed Δ17O(oxidants) O: 38.4 ± 2.0‰, O: 25.6 ± 1.3‰, O: 1.6 ± 0.3‰, O: 0‰
Newly proposed process leading to high Δ17O(SO4 2−)
addition
OH
36%
BrO
49%
O3 (Oterm)
8%
Cl (O2)
7%
DMS
(no oxygen atom)
DMSO
Estimated Δ17O
20.8 − 23.0‰
OH
MSIA
Estimated Δ17O
10.4 − 11.5‰
OH
31%
O3 (Oterm)
69%
MS−
Estimated Δ17O
15.2 − 16.9‰
OH ?
SO4 2−
Estimated Δ17O
11.4 − 12.7‰
Minor
contribution
(~10%?)
abstraction
OH, NO3,
Cl, O3
OH
OH
SO2
Δ17O = 0‰
(assumed)
H2O
isotope equilibrium
with water
in cloud/aerosol
aqueous-phase oxidation
SO2 · H2O
HSO3−
SO3 2−
H2O2
O3 (Obulk)
HOBr (H2O)
SO4 2−
Observed Δ17O
1.3 ± 0.3‰
(DDU)
Estimated Δ17O
0.9 − 1.4‰
(Dome C)
SO4 2−
Observed Δ17O
2.0 ± 0.3‰
(Dome C)
gas-phase oxidation
OH
Recognized processes affecting Δ17O(SO4 2−)

Figure5.

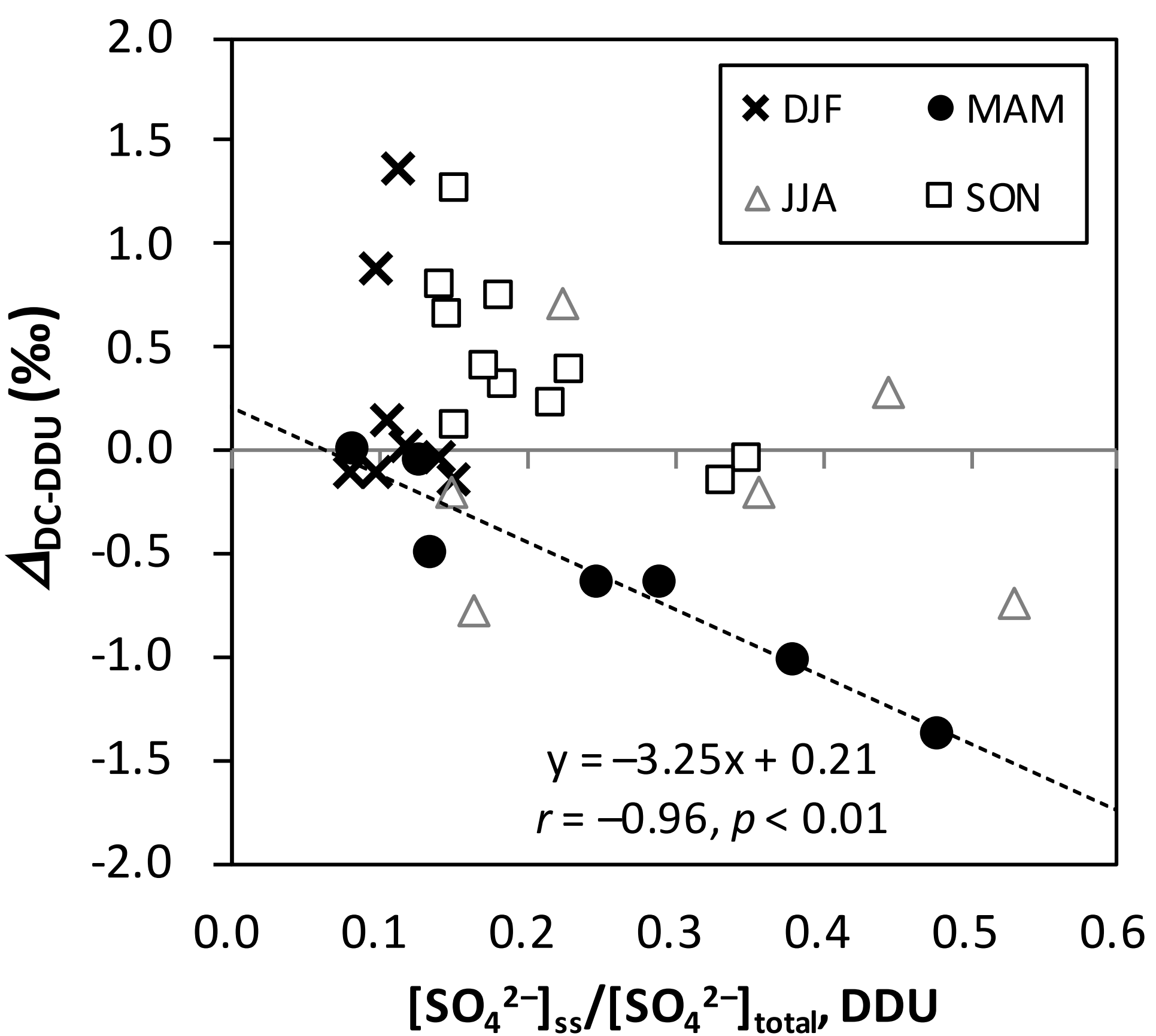
2.0
1.5
1.0
0.5
0.0
-0.5
-1.0
-1.5
-2.0
0.0
0.1
0.2
0.3
0.4
0.5
0.6
DJF
MAM
JJA
SON
y = –3.25x + 0.21
r = –0.96, p < 0.01
Δ DC-DDU (‰)
[SO4 2–]ss/[SO4 2–]total, DDU